Relativistic laser plasma interactions at the University of Michigan

Karl Krushelnick

Center for Ultrafast Optical Science (CUOS)

University of Michigan, Ann Arbor

Experiment

Tony Zhao (student)
Anthony Raymond (student)
Keegan Behm (student)
Thomas Batson (student)
Andrew McKelvey (student)
Paul Campbell (student)
Amina Hussein (student)

Alec Thomas
Louise Willingale
Victor Yanovsky
Anatoly Maksimchuk
John Nees
Gennady Fiksel

Modeling

Chuanfei Dong (student)
Alec Thomas
OSIRIS collaboration (UCLA/IST/USC)

Queen's University of Belfast:
G. Sarri, D. Corvan, D. Doria, B. Dromey, M. Zepf

Imperial College London – Blackett Laboratory:
M. Bloom, K. Poder, J. Cole, S.P.D. Mangles, Z. Najmudin

Outline:

1. Center for Ultrafast Optical Science (CUOS)

2. X-ray Generation from laser wakefield acceleration

   X-ray optimization

   Femtosecond phase contrast imaging

   Femtosecond absorption spectroscopy

3. K-alpha imaging

   Relativistic reconnection

4. Pion production

CUOS laser systems

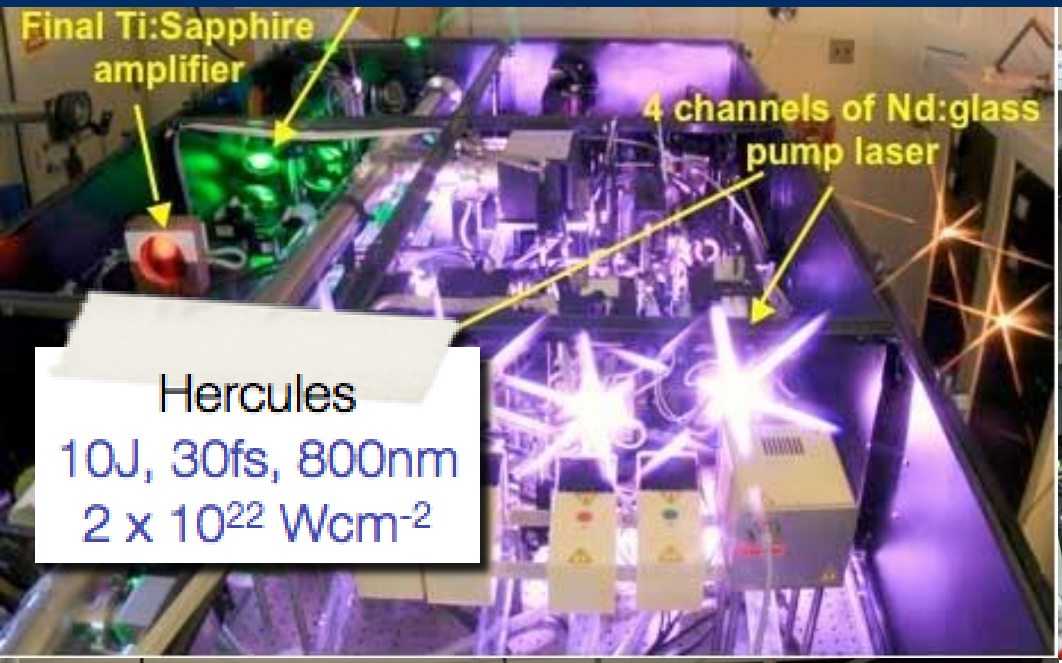

Hercules
10J, 30fs, 800nm
2×10^{22} Wcm^{-2}

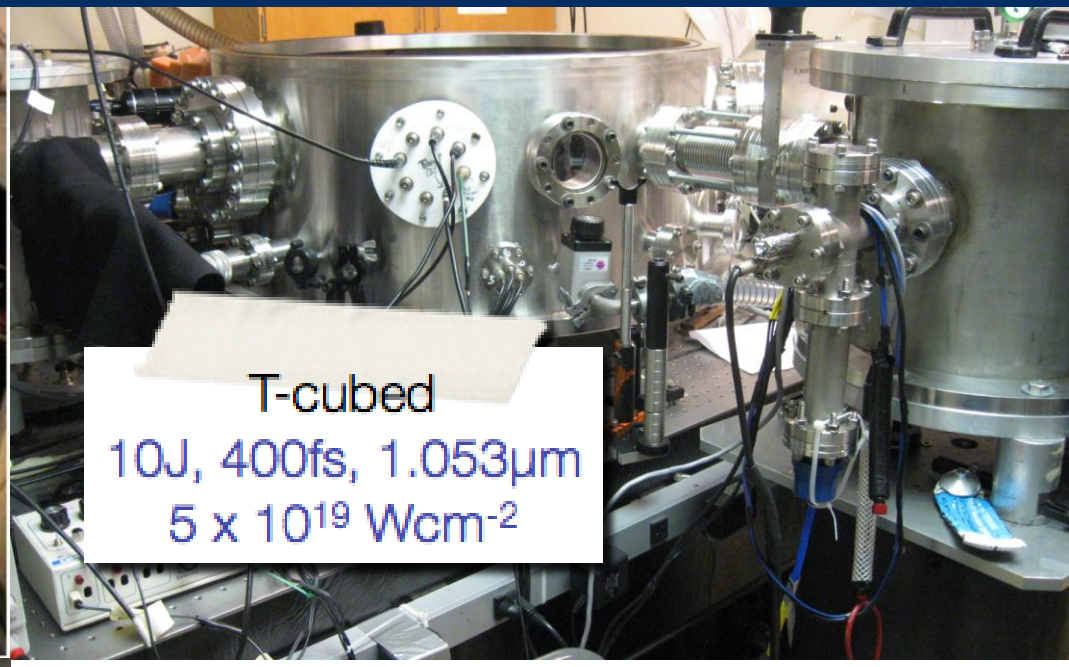

T-cubed
10J, 400fs, 1.053μm
5×10^{19} Wcm^{-2}

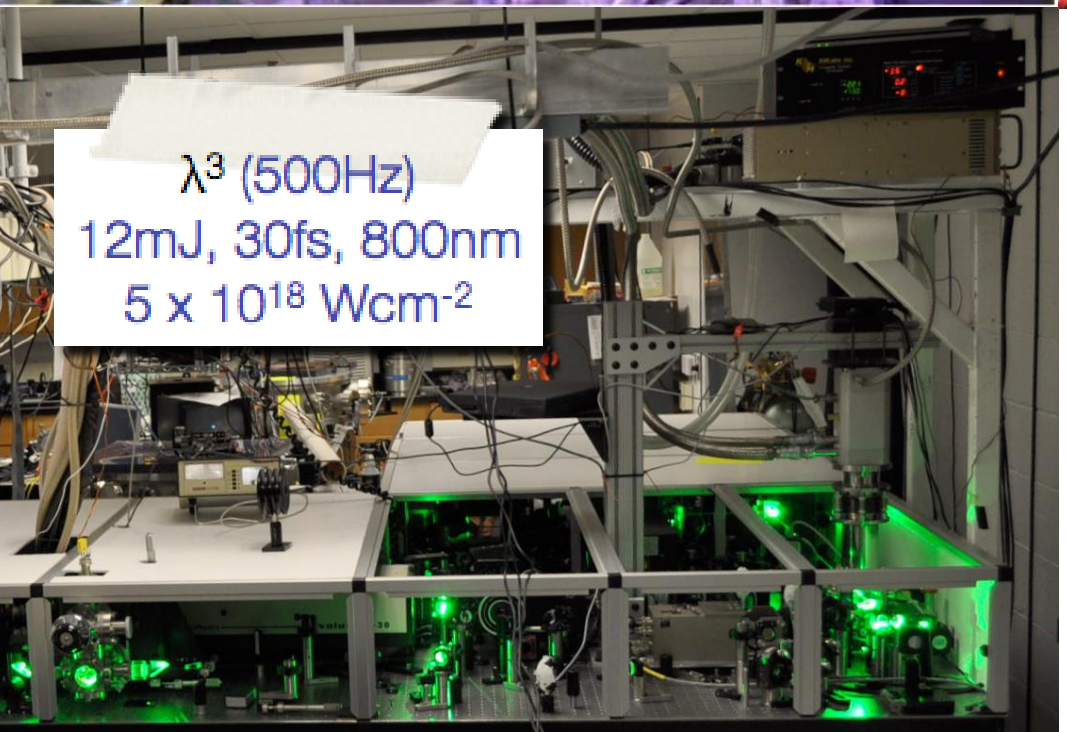

λ^3 (500Hz)
12mJ, 30fs, 800nm
5×10^{18} Wcm^{-2}

External laser systems

Omega EP
<1000J, 1-10ps, 1.053μm
1×10^{19} Wcm^{-2}

Titan
<300J, 1-10ps, 1.053μm
5×10^{19} Wcm^{-2}

Gemini
2x15J, 30 fs, 800nm
~10^{21} Wcm^{-2}

Laser Radiation sources at CUOS

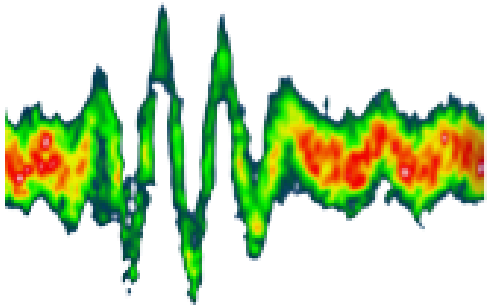

High Order Harmonic pulse generation
Dollar (PRL 2013)
Easter (NJP 2013)

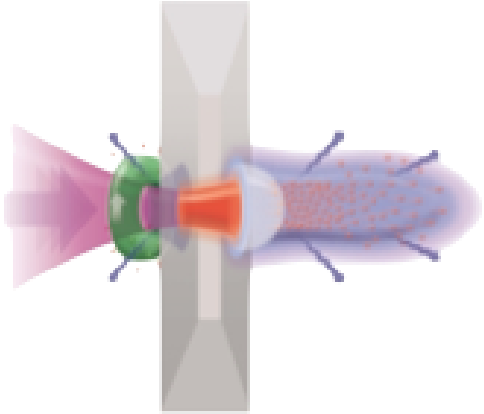

Laser acceleration of ions
Dollar (PRL 2011,2012)
Dollar (APL 2103)

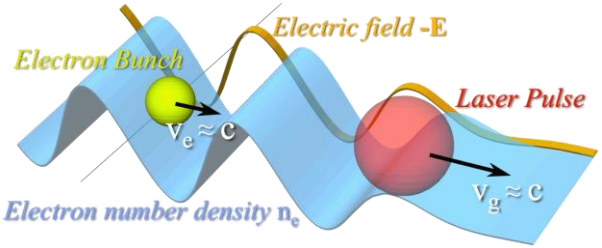

Laser wakefield acceleration
Schumaker (PRL 2013)
He (Nat. Comm. 2015)

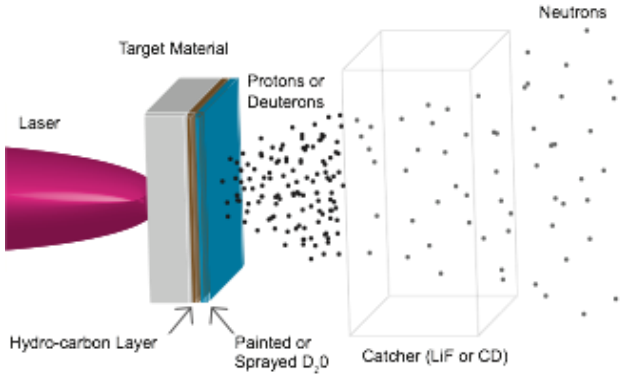

Directional high energy neutron beams
Zulick (APL 2014)

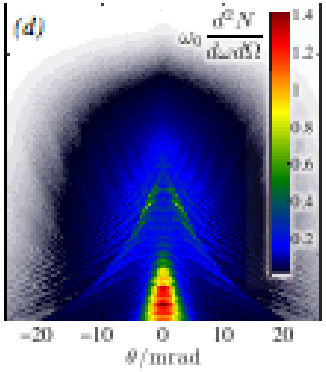

Table-top x-ray and γ ray sources
Kneip (Nat. Phys. 2010)
Sarri (PRL 2014)

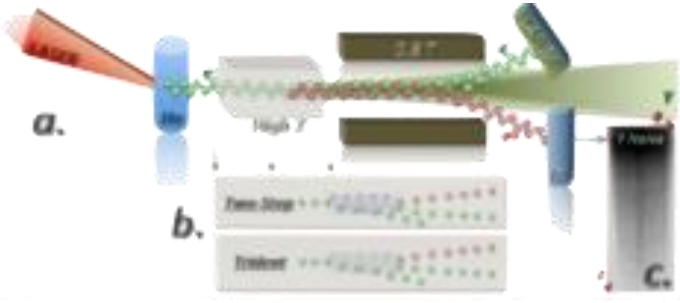

Positron beams
Sarri (PRL 2013)
Sarri (Nat. Comm. 2015)

X-ray Generation from laser acceleration

Femtosecond phase contrast imaging, femtosecond absorption spectroscopy

Experimental Setup: Gas Cells - HERCULES

10mm Gas Cell

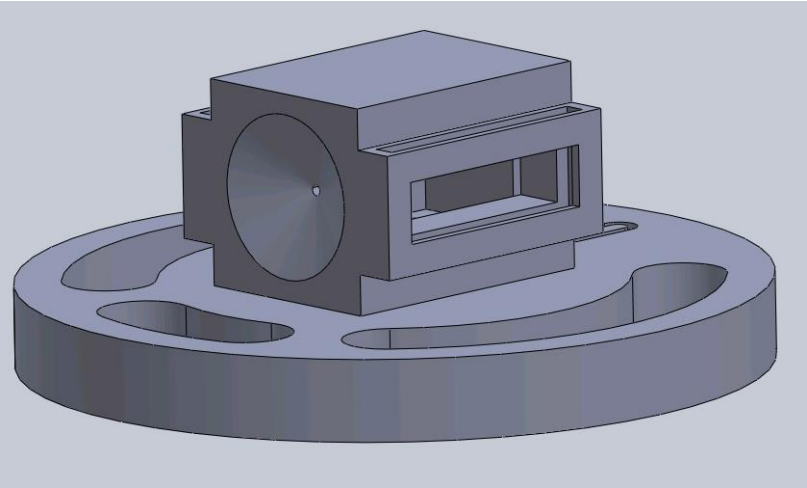

Experimental Parameters

Laser	100 TW, 30fs, 800nm Ti:Sapphire
Focusing Optic	f/20
Spot Size	~20µm
Gas Jet	10mm Gas Cell
Gas Mix	Ionization injection: 1.25%N Self Injection: Pure He
Density	~10^{19} cm^{-3}

Betatron X-ray generation

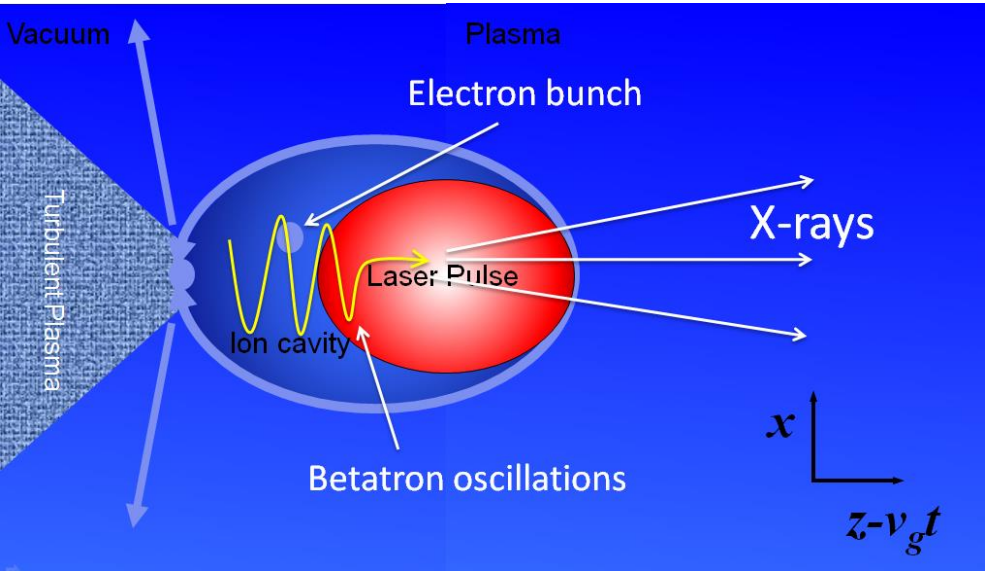

- In lab frame, radiation has fundamental wavelength:

$$\lambda_{\mathrm{LWFA}} \approx \frac{\sqrt{2}\pi c}{\gamma^{3/2}\omega_p} = \frac{\lambda_p}{\sqrt{2}\gamma^{3/2}}$$

- and harmonics which peak at photon energy of nearly:

$$E_c = \hbar \frac{6\pi^2\gamma^3 c r_0}{\lambda_b^2} = 6keV$$ for 270 MeV, $5\times10^{18}\mathrm{cm}^{-3}$.

[1] E. Esarey, et al. *Phys. Rev. E* **65**, (2002).
[2] A.G.R. Thomas. *Phys. Plasmas* **16**, (2009).
[3] A.G.R. Thomas. *Phys. Plasmas* **17**, (2010).

Experimental Setup and Parameters

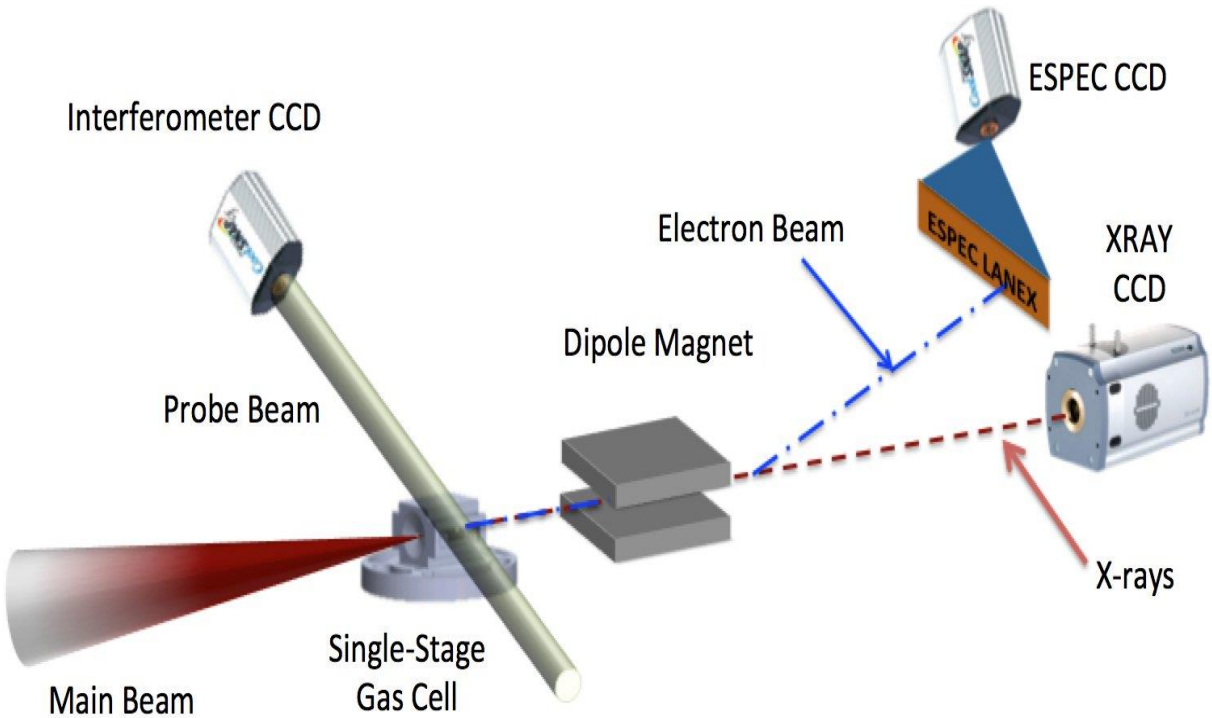

HERCULES Laser	2 J, ~34 fs, ~2 x 10^{19} W/cm^2
Focusing Optic	f/20
Spot Size	~26 µm
Gas Cell	Single stage; either 3 or 5 mm
Gas Mix	2.5% N, 97.5% He or pure He
Electron Density	0.8 – 2.2 x 10^{19} cm^{-3}

HERCULES Gas Cell: Energy

10 Consecutive Shots 10mm Gas Cell

1.25%N 98.75%He

2psi

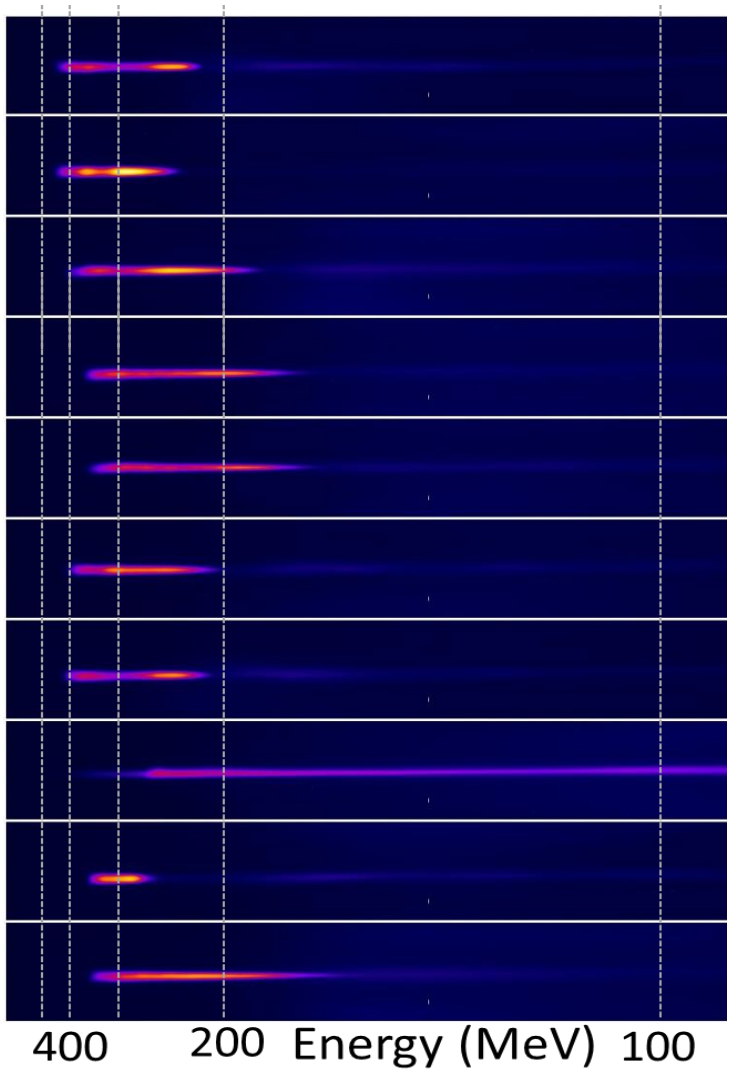

Pure He

2.5psi

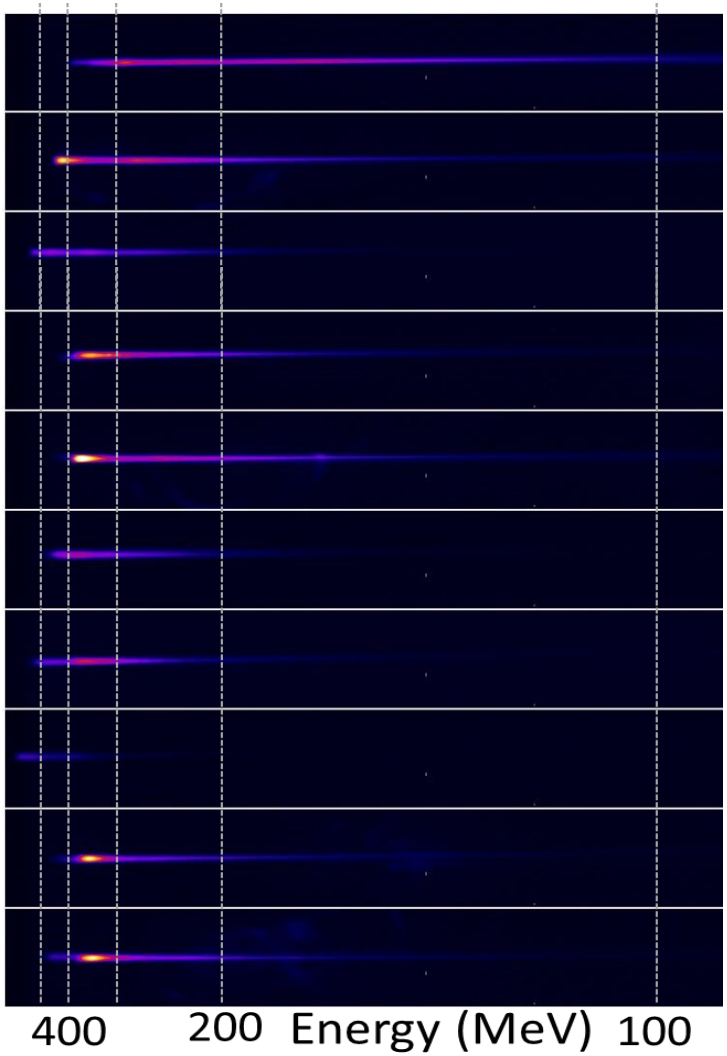

Betatron X-ray generation (single shot spectra)

(shows synchrotron structure)

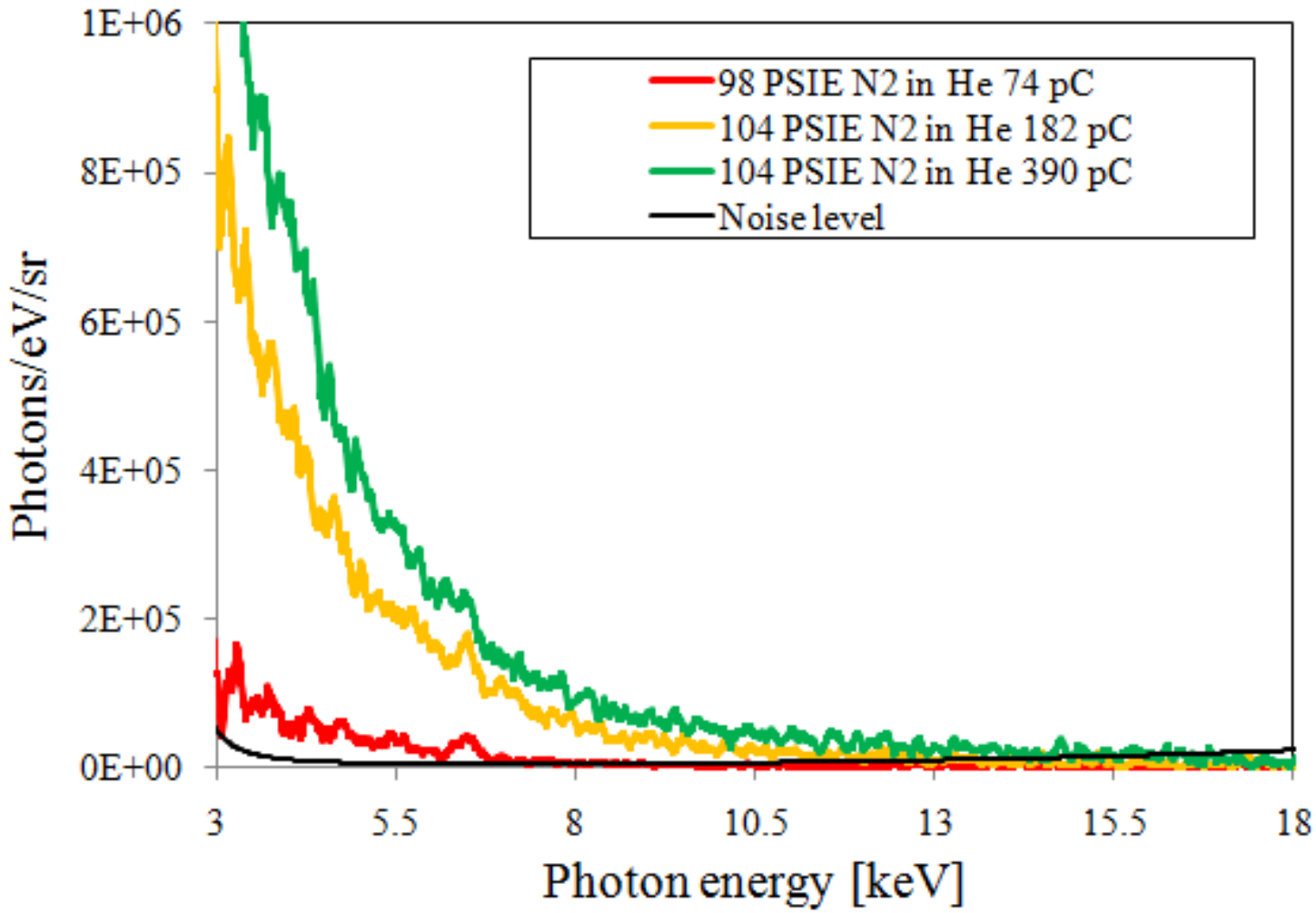

Control of Betatron flux, spatial coherence, spectrum

1) Laser pulse shape (temporal/spatial)
   - chirped pulses
   - focal spot shape (affects bubble shape), multiple spots
2) Electron injection process
   - self-injection/ionization injection
   - “off axis” beams/ beam driven versus laser driven
3) Propagation distance (beam instabilities affcet x-ray generation)
   - laser interaction increases x-ray flux
   - e-beam instabilities increase x-ray flux

Pulse Measurements

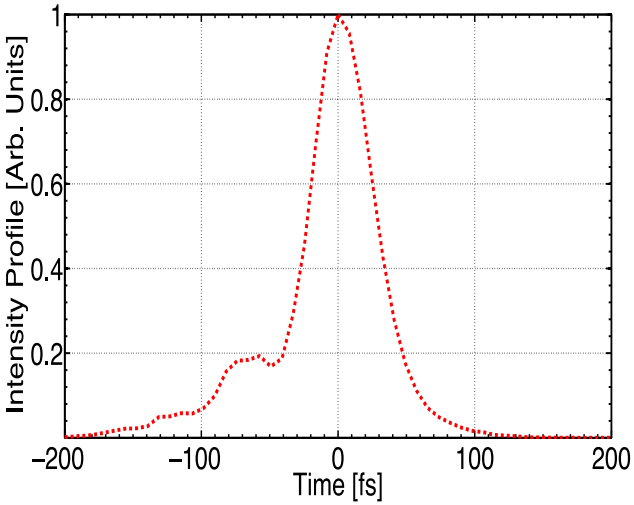

(a) Positively chirped pulse

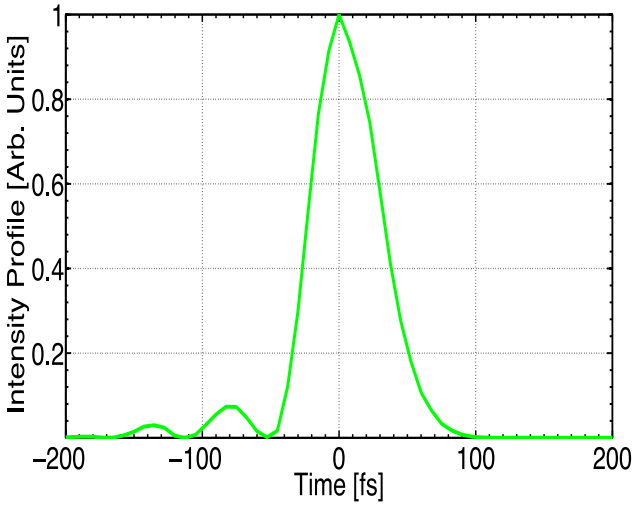

(b) Optimally compressed pulse

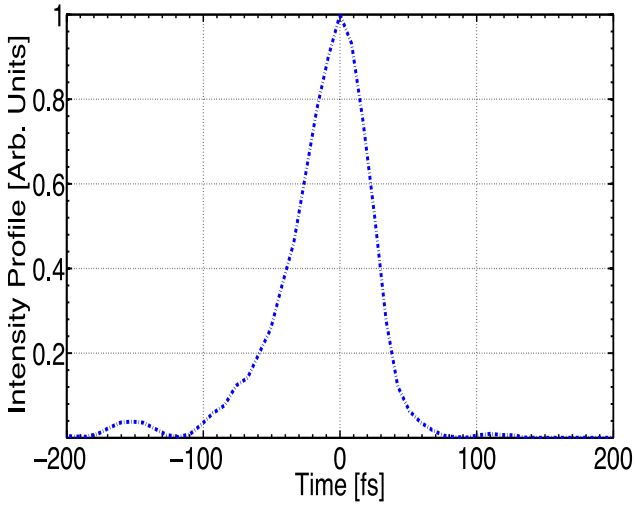

(c) Negatively chirped pulse

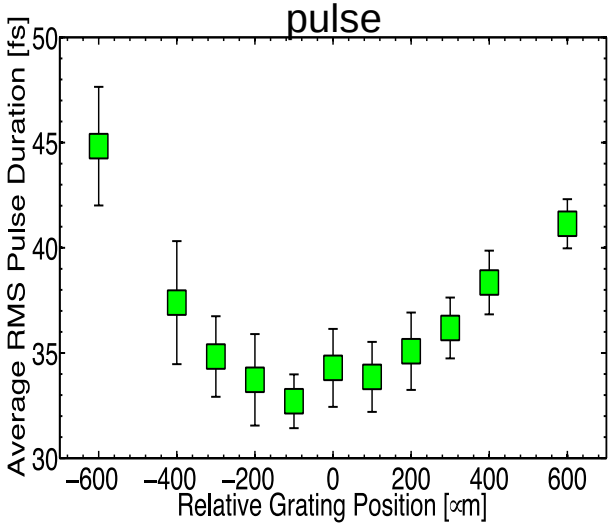

(d) Pulse duration vs. relative grating position

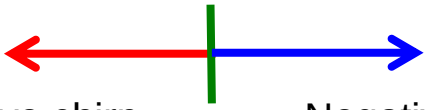

Positive chirp Negative chirp

Electron Charge and X-ray Flux

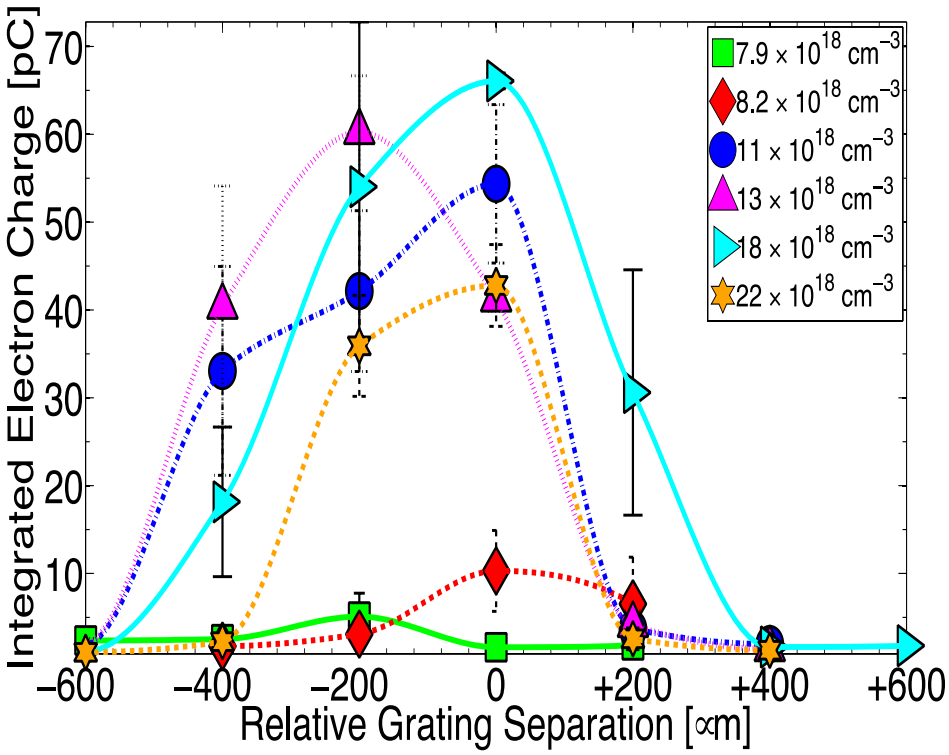

Positive chirp Negative chirp

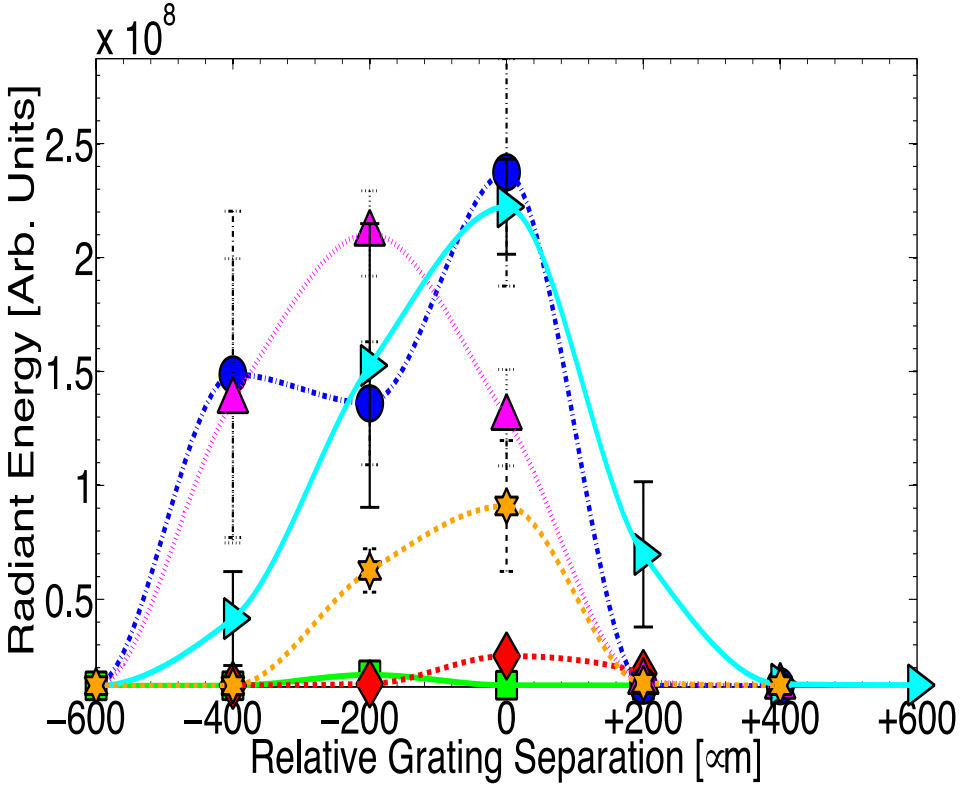

Positive chirp Negative chirp

Experimental Results:
Electron Images with Ring Structure

a) Magnetic spectrometer images

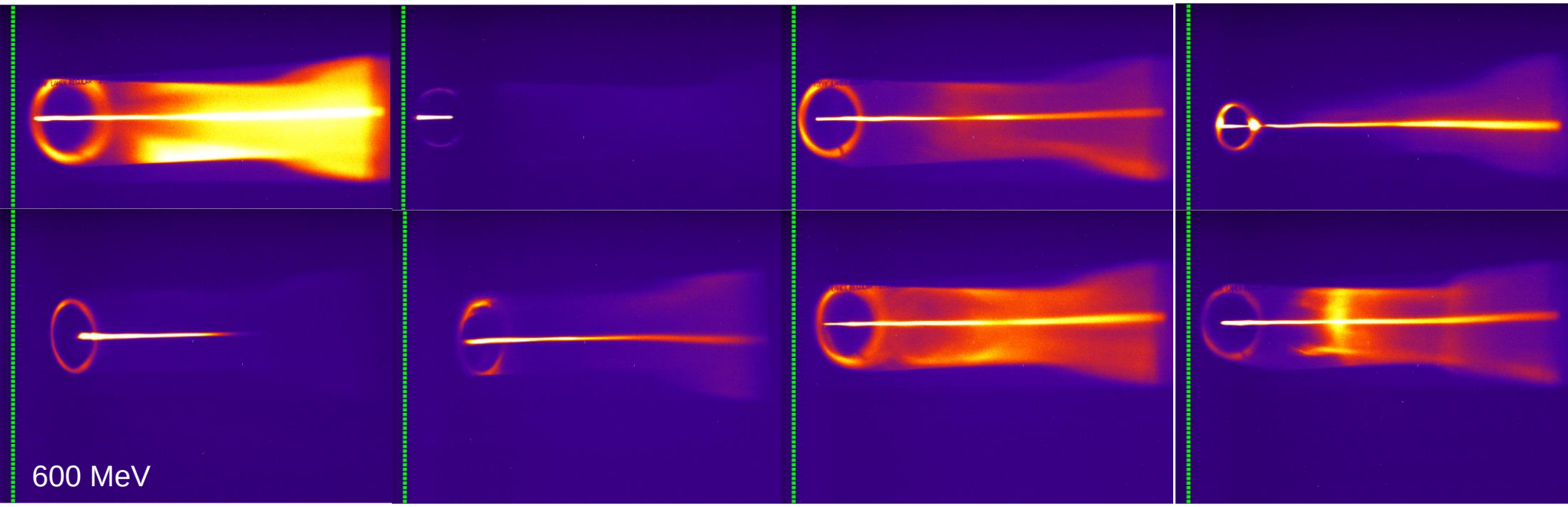

b) On-axis profile images

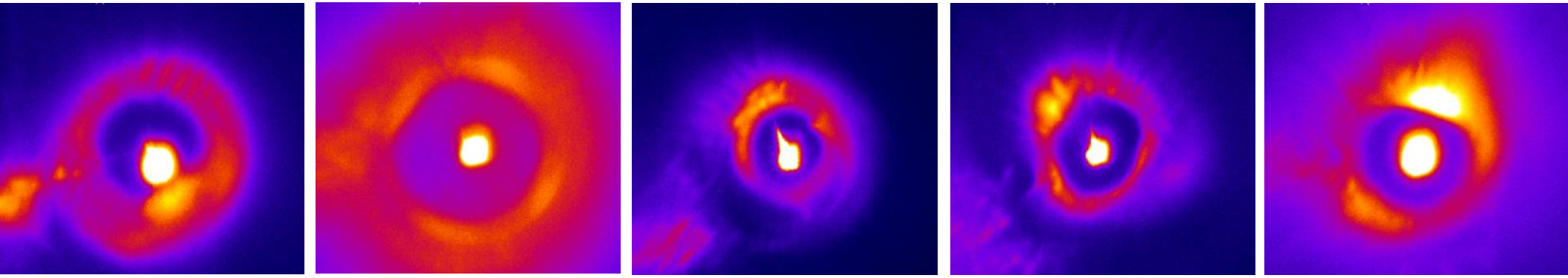

[3] B. B. Pollock, APS: BAPS.2013.DPP.UO7.1

Halo causes significant increase in X-ray Flux

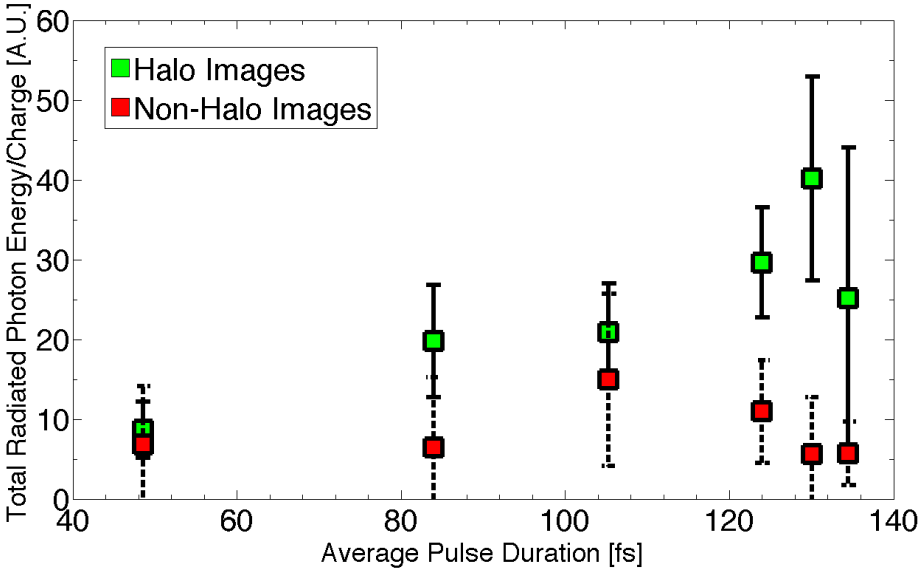

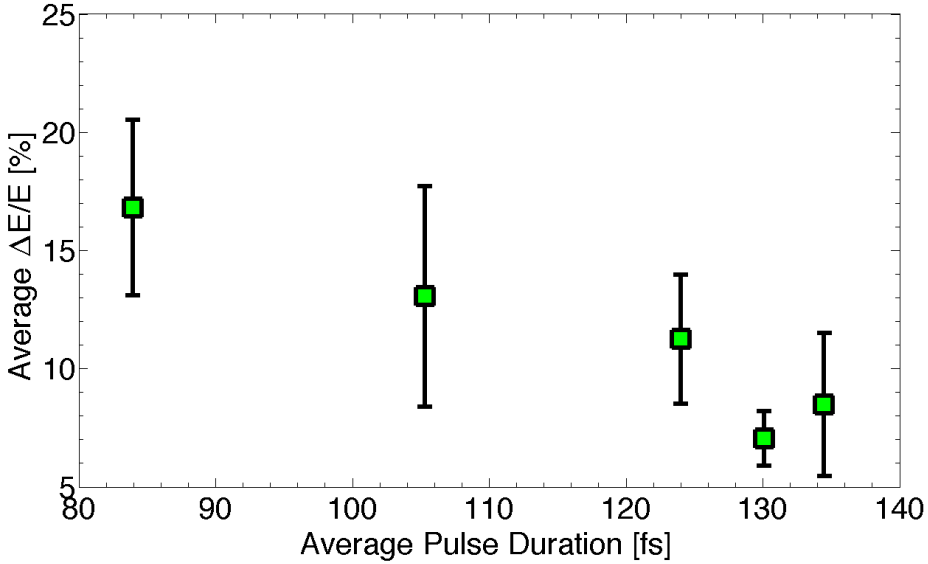

a) Total radiated photon energy per unit charge vs. Pulse duration

b) Average halo energy spread vs. Pulse duration

Use betatron x-rays for time resolved absorption spectroscopy

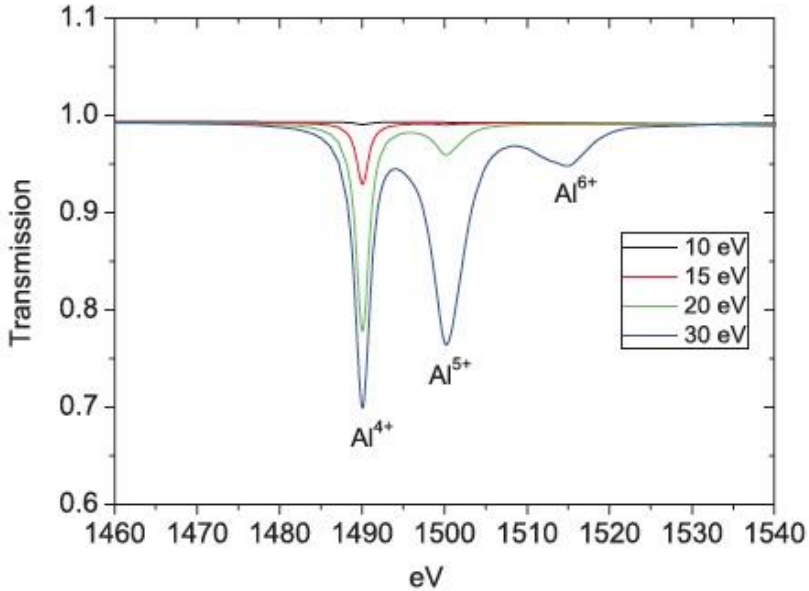

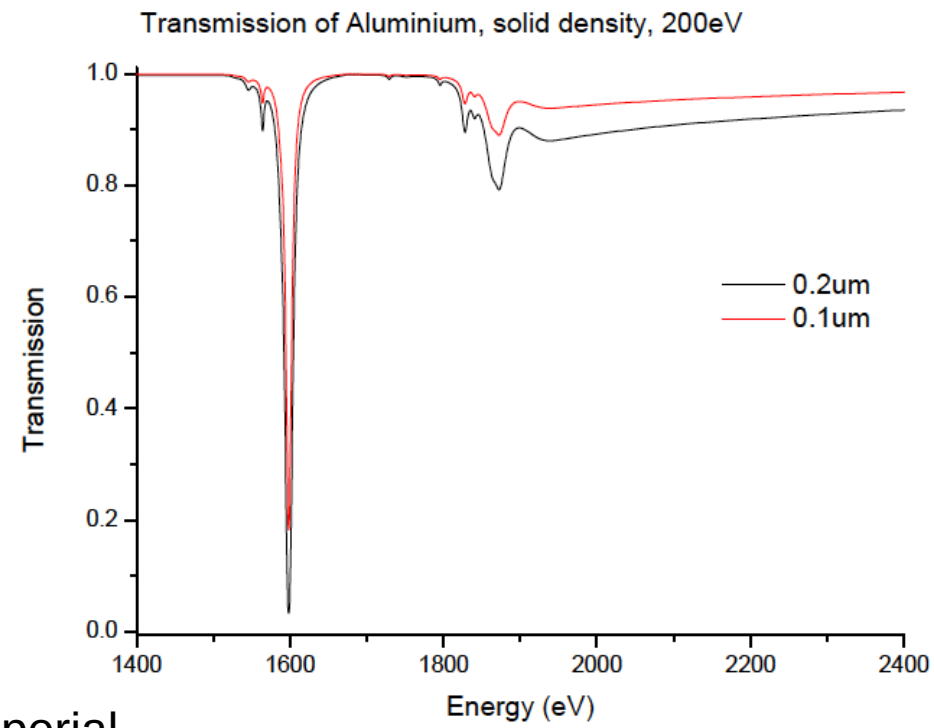

Calculations by Ed Hill, Steve Rose, Imperial College

Experimental Setup

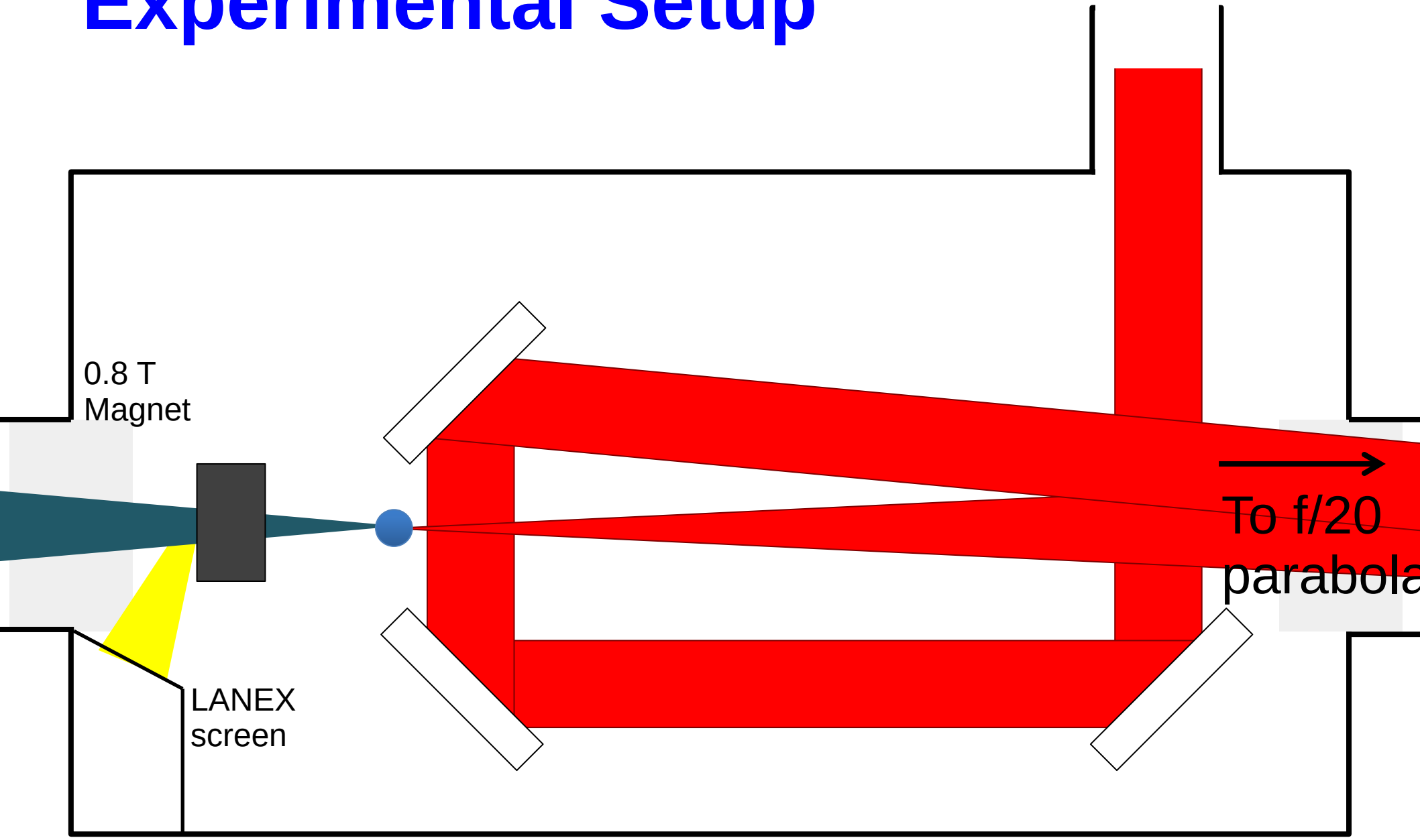

Experimental Setup

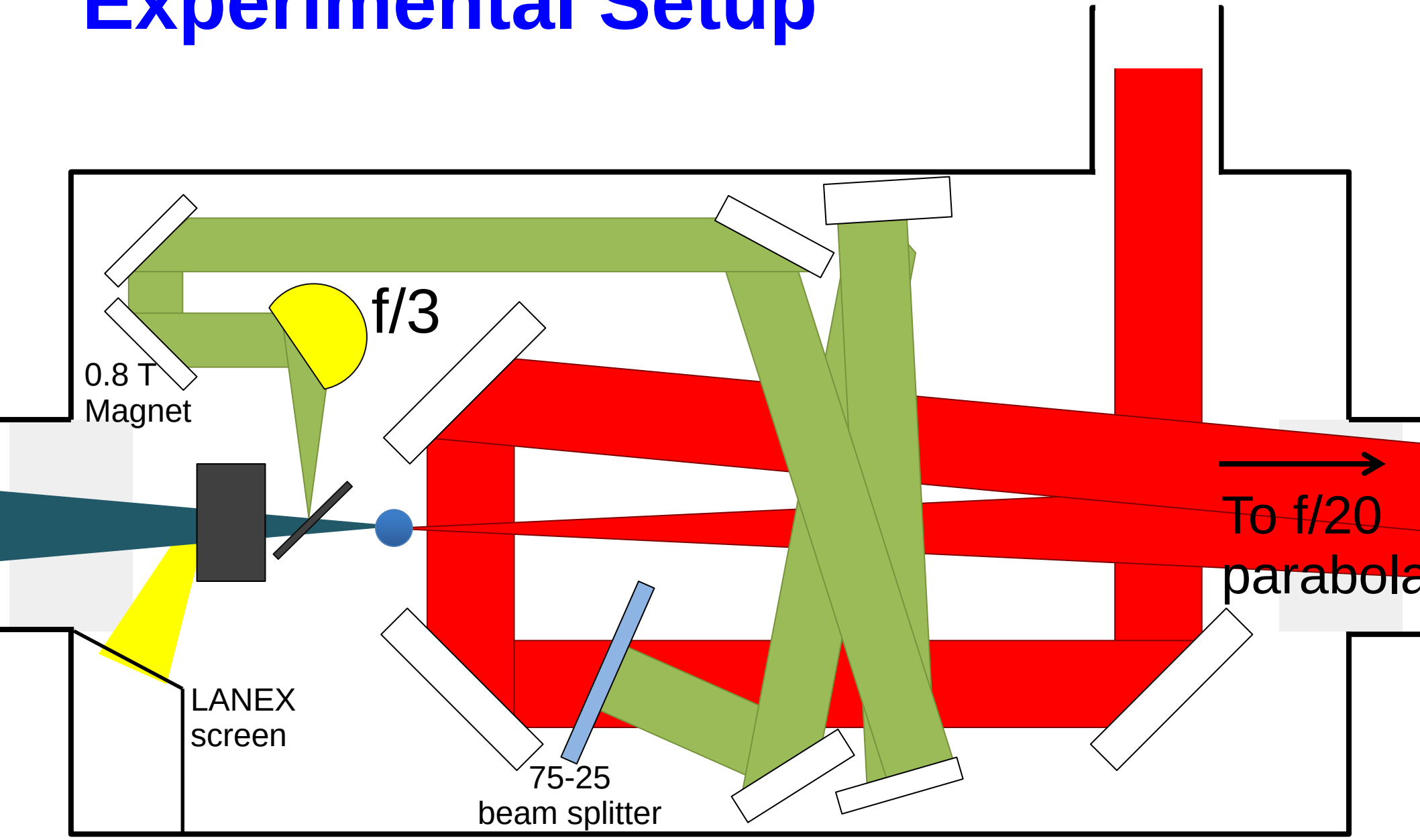

Experimental Parameters

70 TW → 50 TW for LWFA, 20 TW for heater beam

Solid target is 4 μm aluminum

Intensity of wakefield beam ~ 5 x 10^{18} W/cm^2

Intensity of heater beam on target ~ 1.0 x 10^{16} W/cm^2

ANDOR iKon-M CCD camera to measure x-rays in the single photon regime.

Obtain a spectrum by converting "counts" into a specific photon energy across the chip.

Calibration of the camera with an ^{55}Fe source indicates a limiting resolution of ~300 eV.

Double hits can significantly distort the high energy component of the spectrum for higher occupancy.

Occupancy = λ = 31.13%

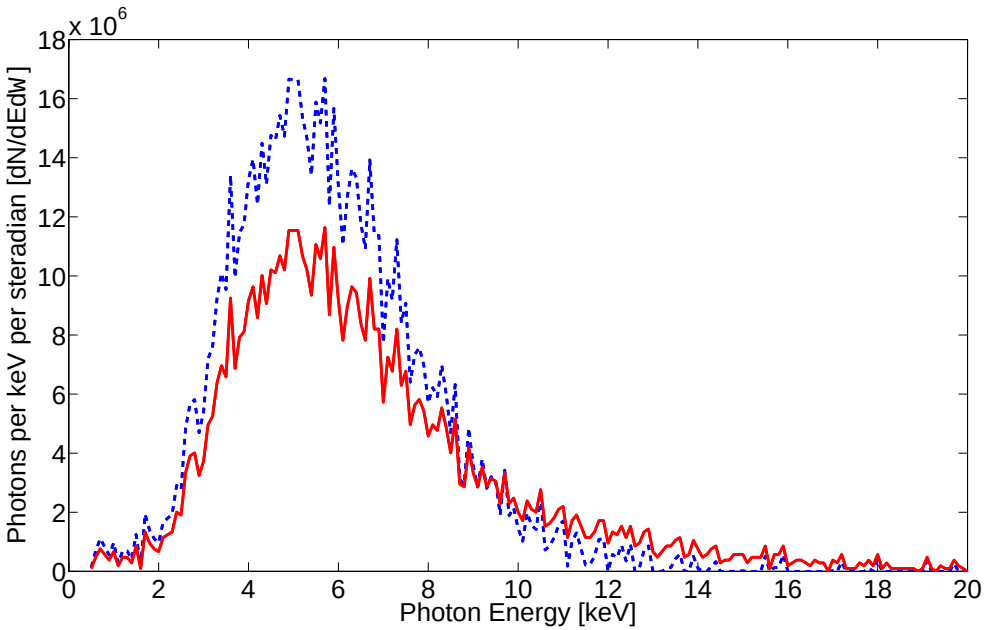

$$P(n) = \frac{\lambda^n e^{-\lambda}}{n!} \qquad \frac{P(2)}{P(1)} = \frac{\lambda^2 e^{-\lambda} 1!}{\lambda e^{-\lambda} 2!} = \frac{\lambda}{2}$$

- Applied convolution algorithm to data to determine the probability of double hit events and corrected the spectrum for such events.
- Used Monte Carlo simulations to determine the upper occupancy limit that can still be corrected.

Raw spectra before double hits correction is applied and after double hits correction.

$$\lambda = \frac{\text{pixels with signal}}{\text{total pixels}} = \text{mean signal count per pixel}$$

Solid Target Alignment

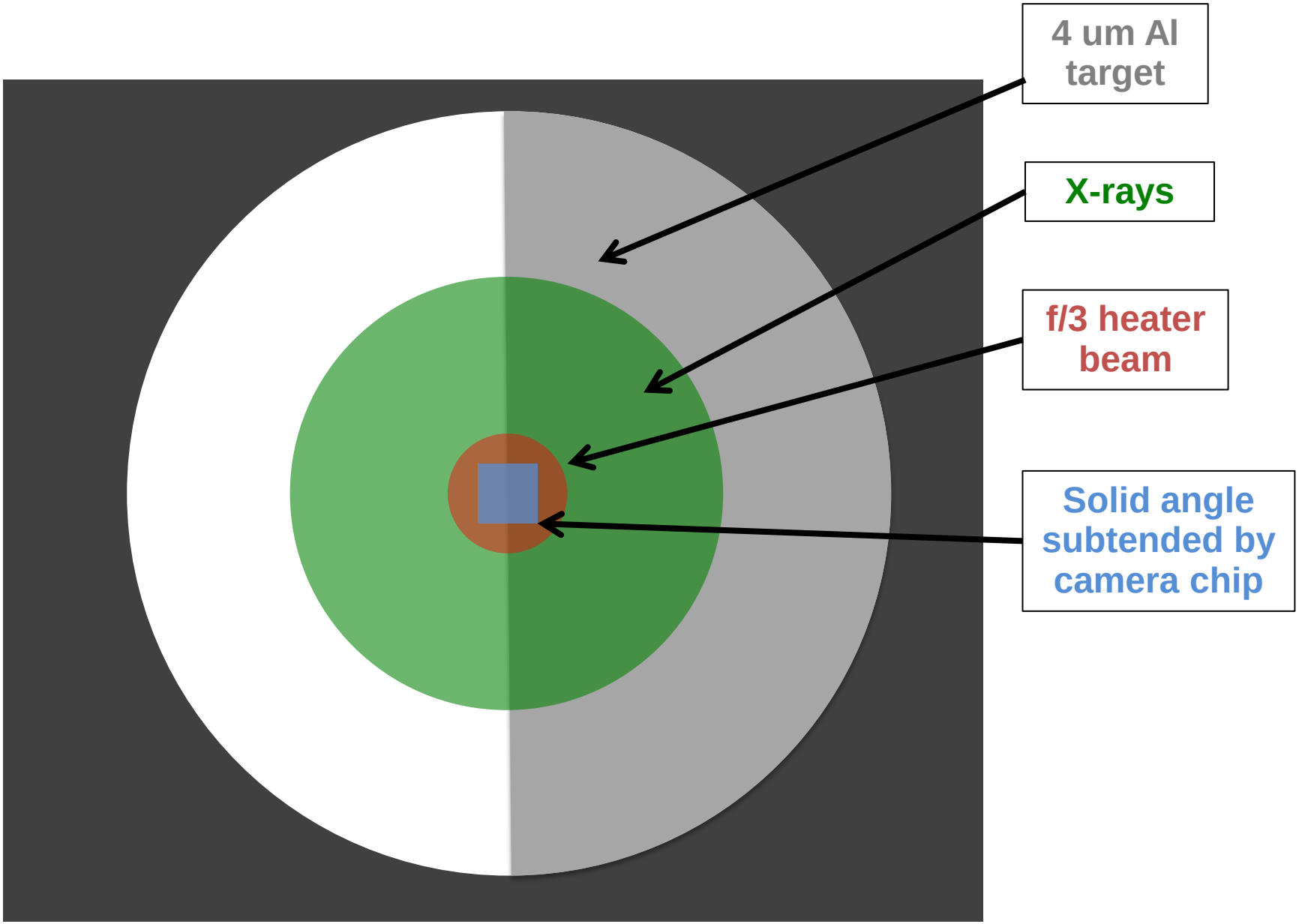

Data Analysis

A typical image from the CCD camera shows the projection of the Al foil onto our chip.

Selecting a region of interest about each half of the image allows us to create an Al-absorption spectrum and a reference spectrum on each shot.

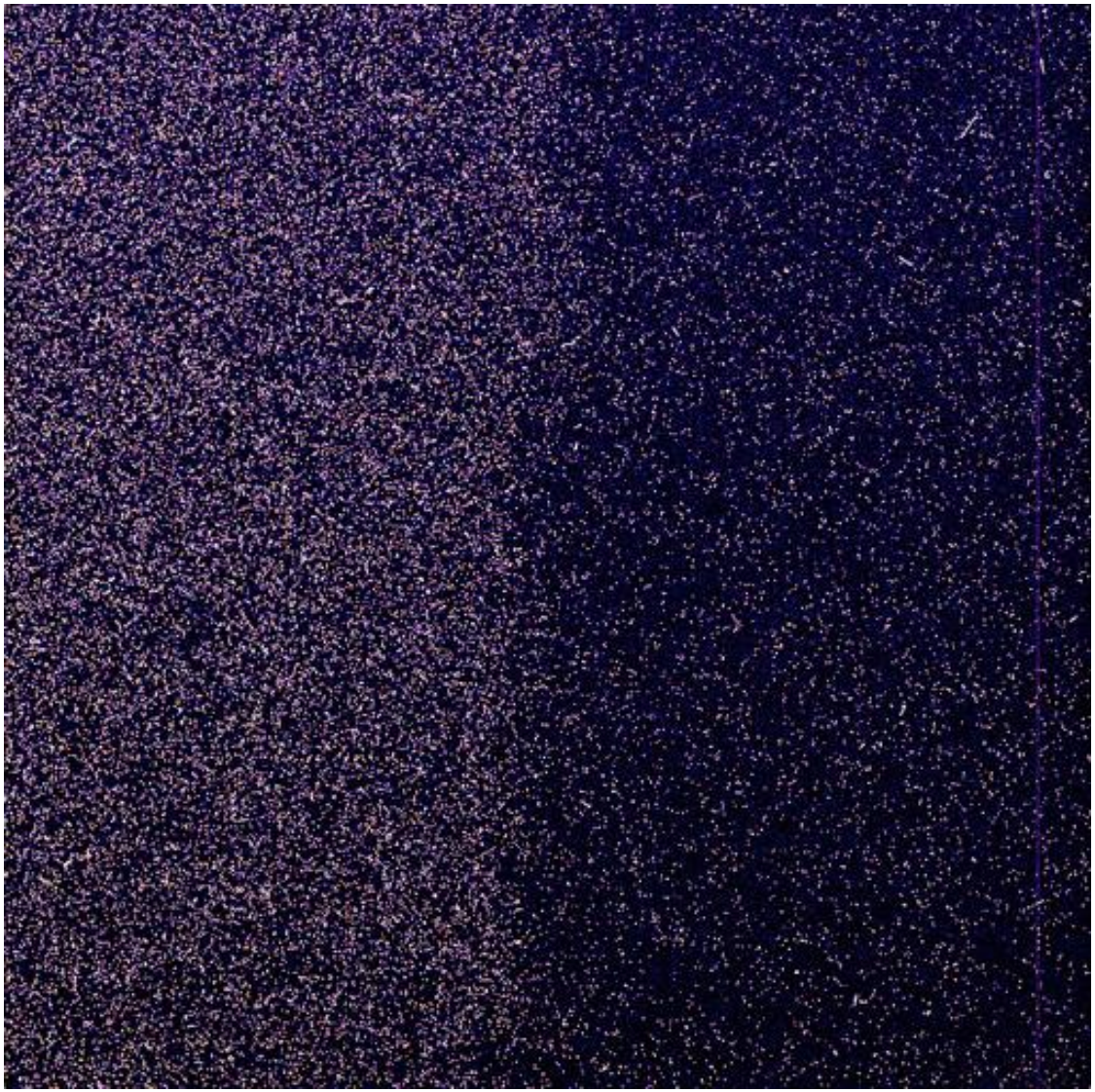

Data Analysis

A typical image from the CCD camera shows the projection of the Al foil onto our chip.

Selecting a region of interest about each half of the image allows us to create an Al-absorption spectrum and a reference spectrum on each shot.

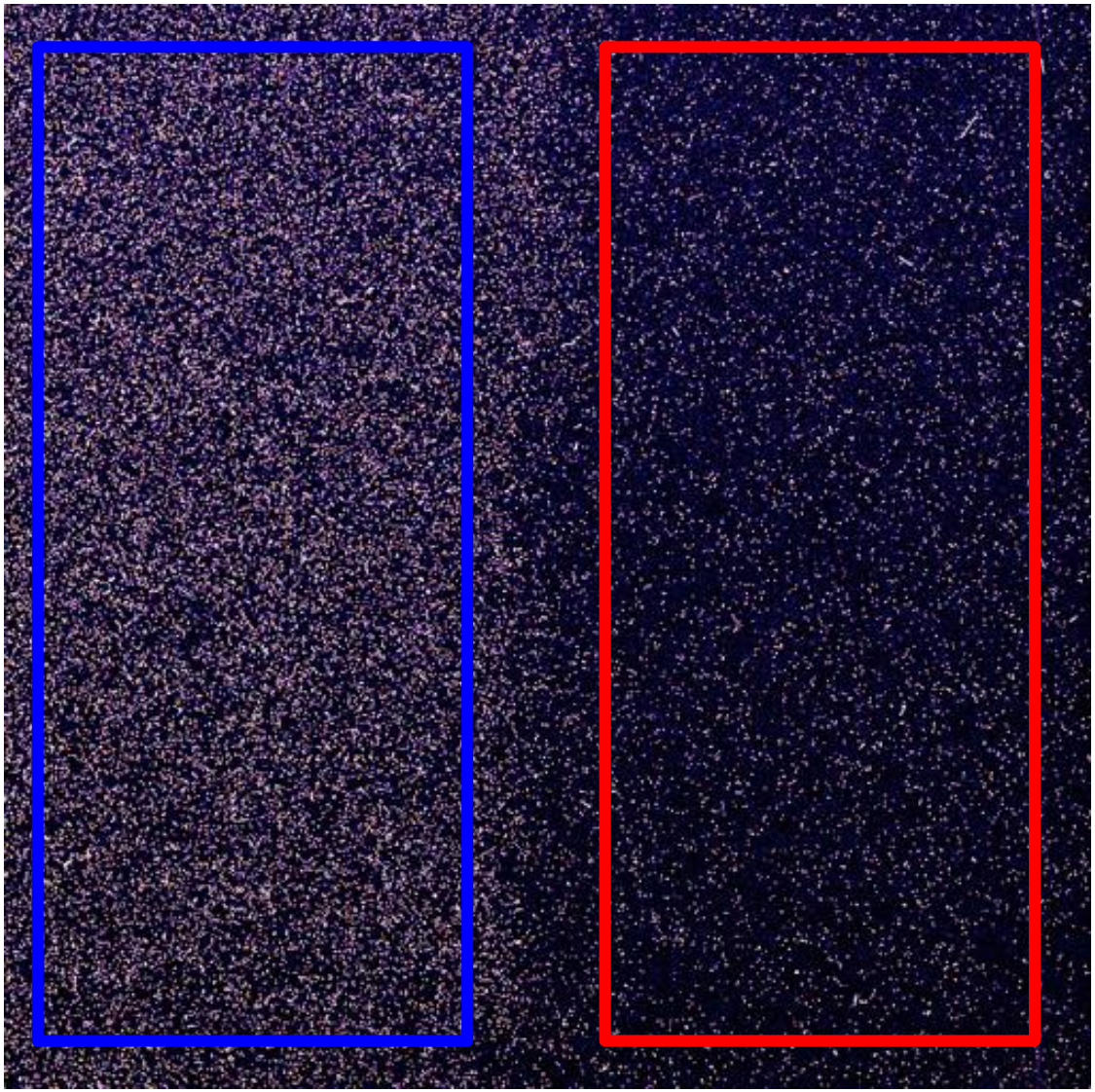

Data Analysis

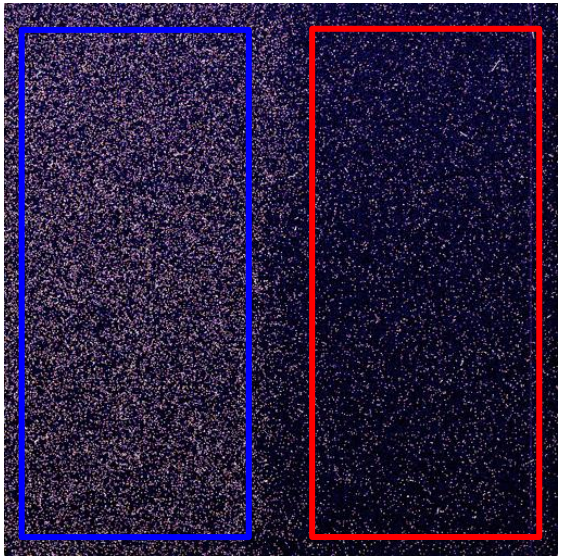

Data Analysis

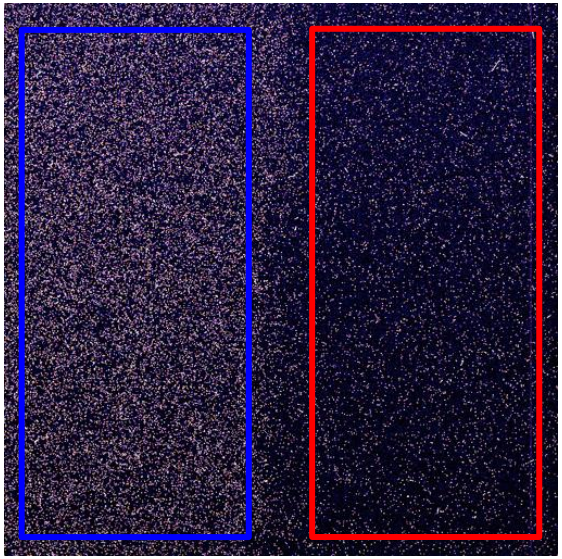

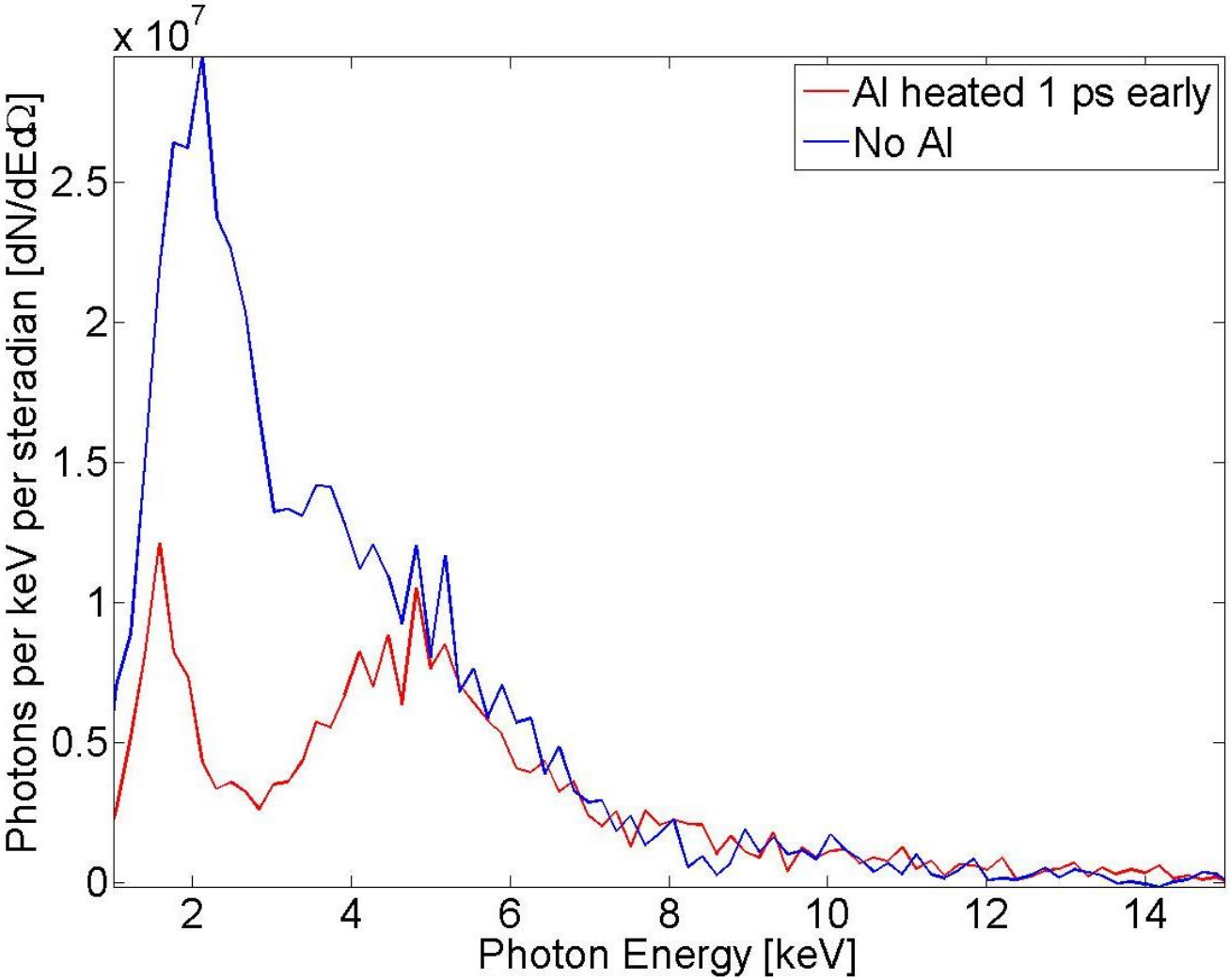

Heating the Al causes the K-edge to shift to higher energies

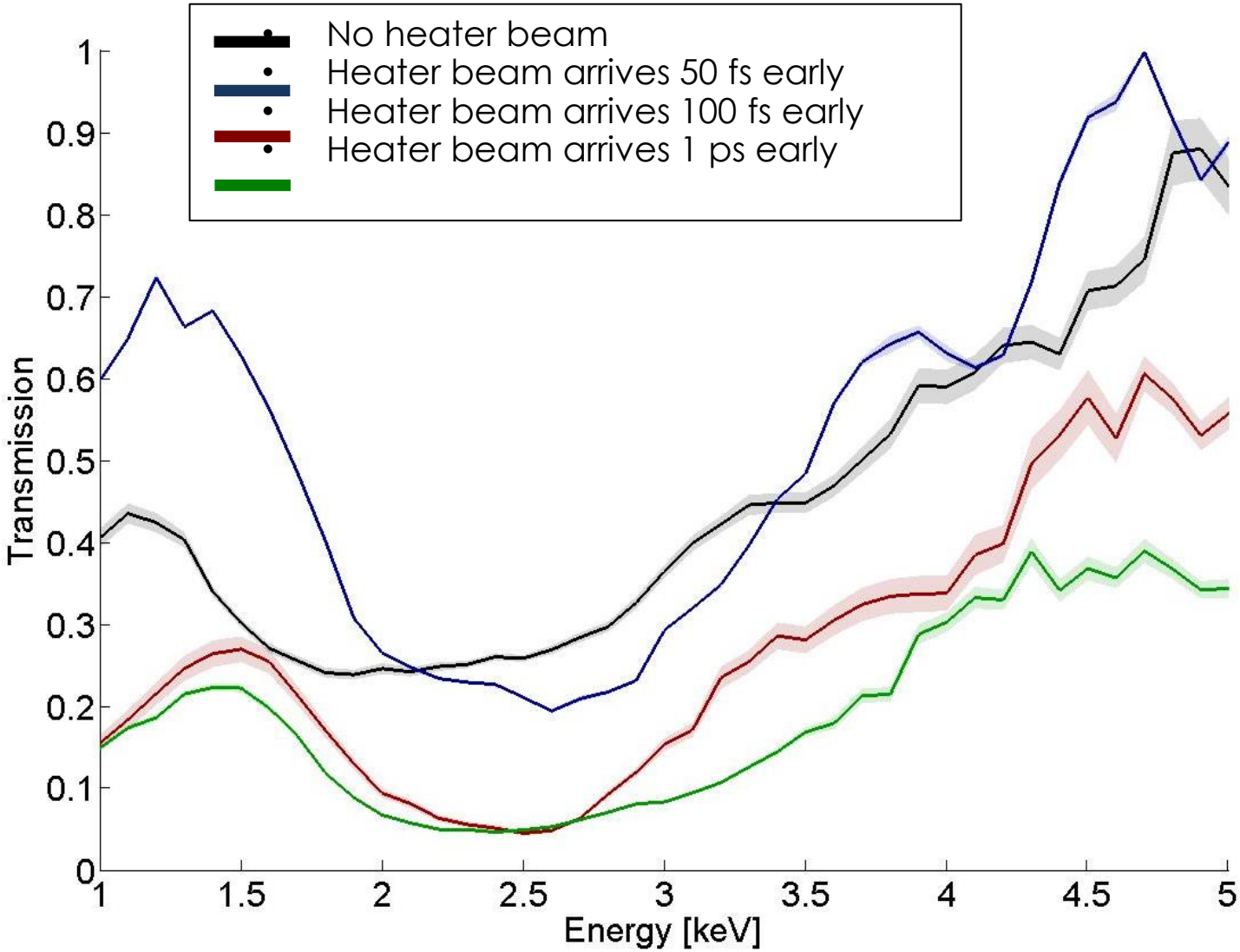

Betatron Phase-Contrast Experimental Setup

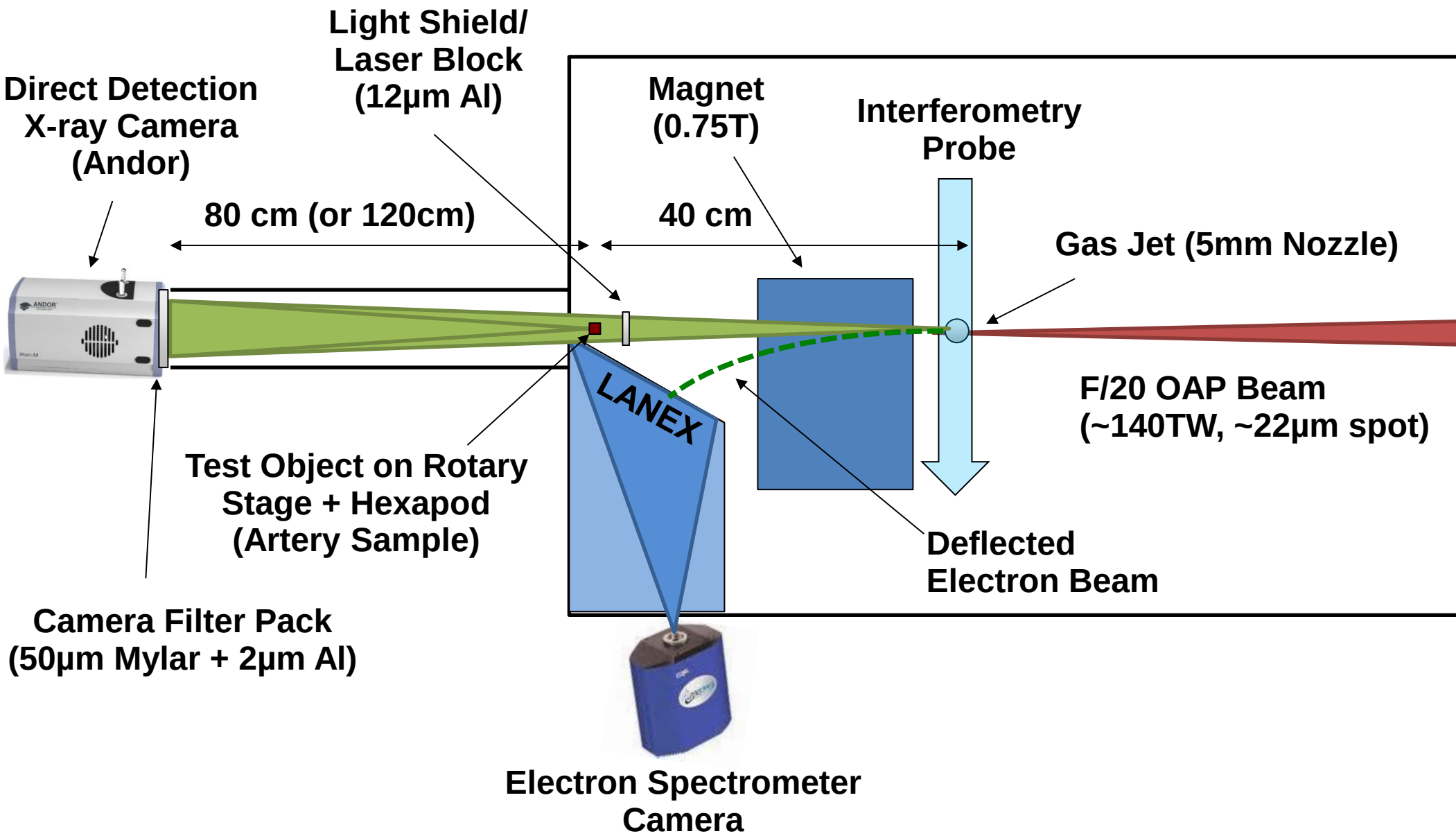

Phase contrast imaging with the x-ray source

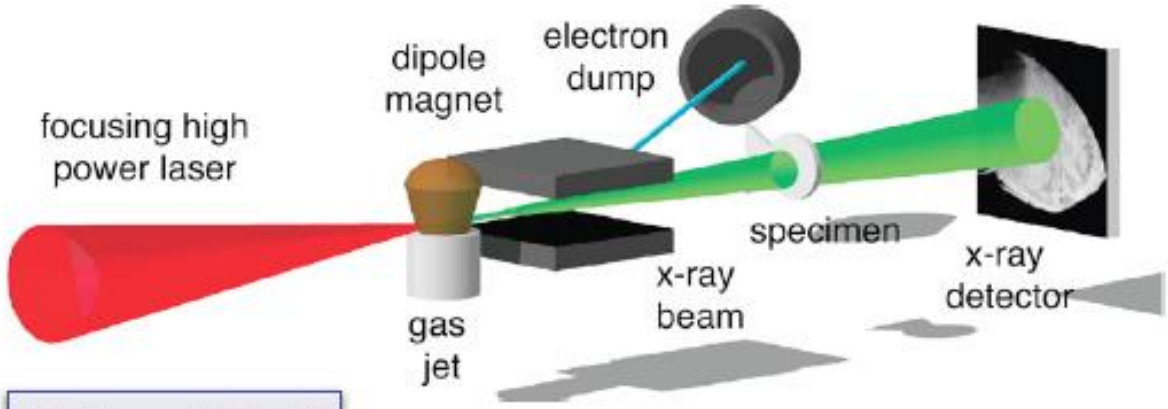

Ecrit ≈ 10keV

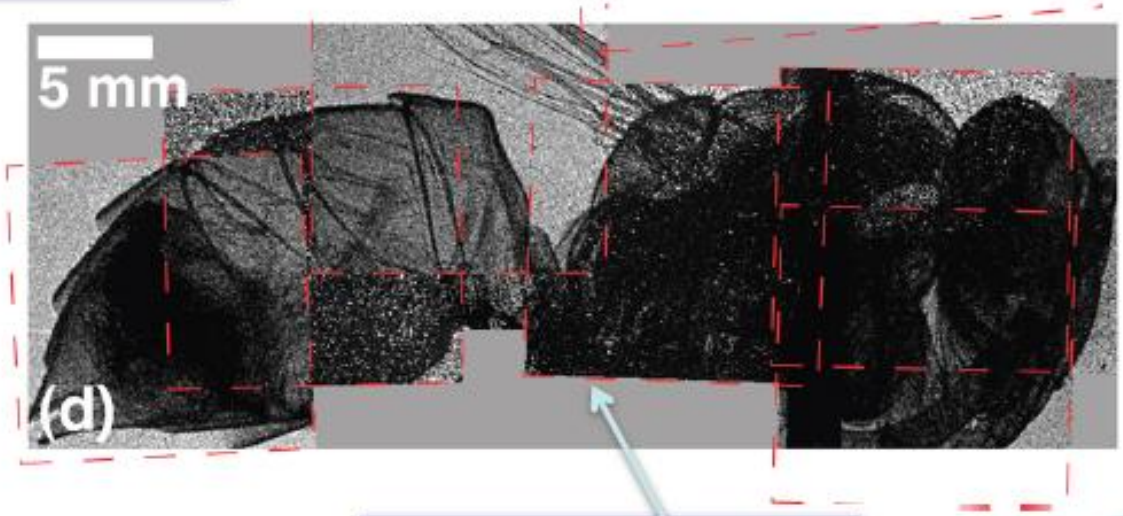

Phase contrast images

Absorption contrast imaging

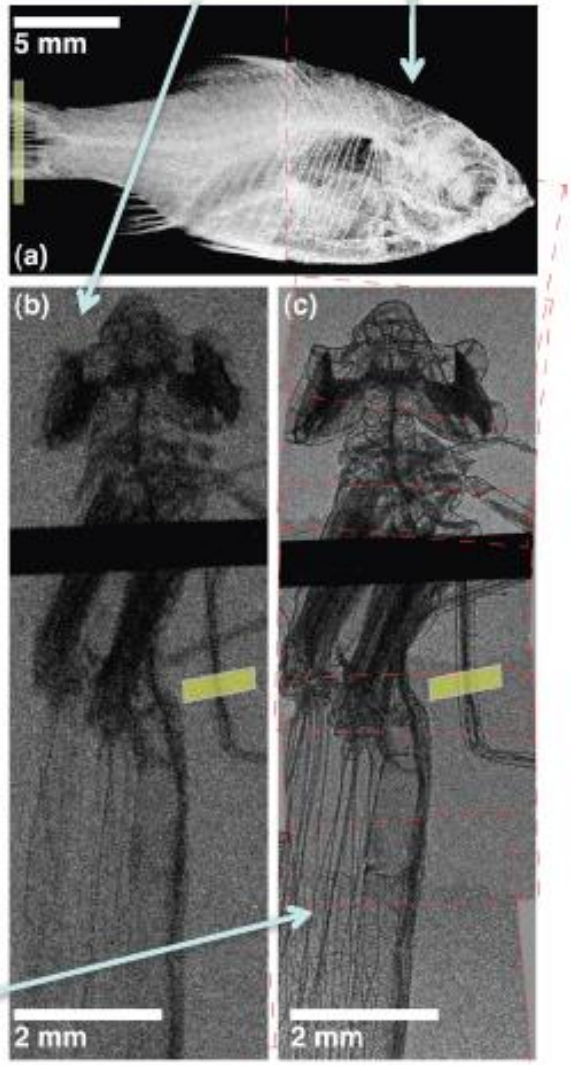

S Kneip et al, APL, 99, 093701 (2011)

Radiography & Phase Contrast Imaging

(with Massachusetts General Hospital)

Artery Sample in Paraffin Wax

Side View Photograph

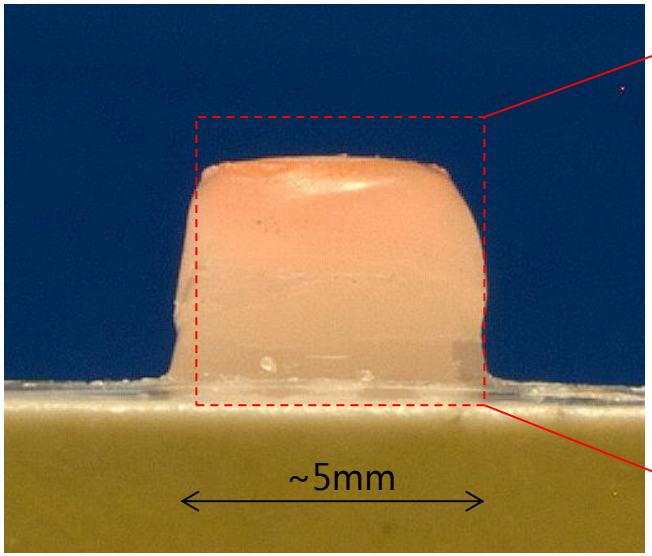

Radiograph

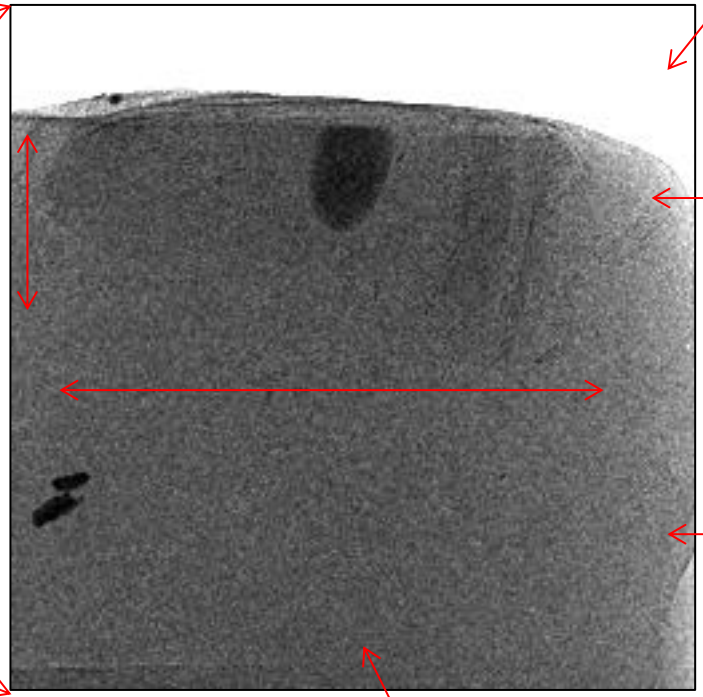

Straight-through (20000+ counts, saturated)

Arterial Plaque (dark spot)

Artery (dark area)

Metal Shaving on Surface (dark spot)

Sample Signal (~4000 counts)

Top View Photograph

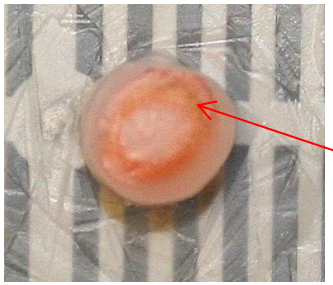

Arterial Plaque Build-up

Images Normalized

K-alpha imaging -

Fast electron dynamics and relativistic reconnection

Experimental setup for Cu K_α imaging

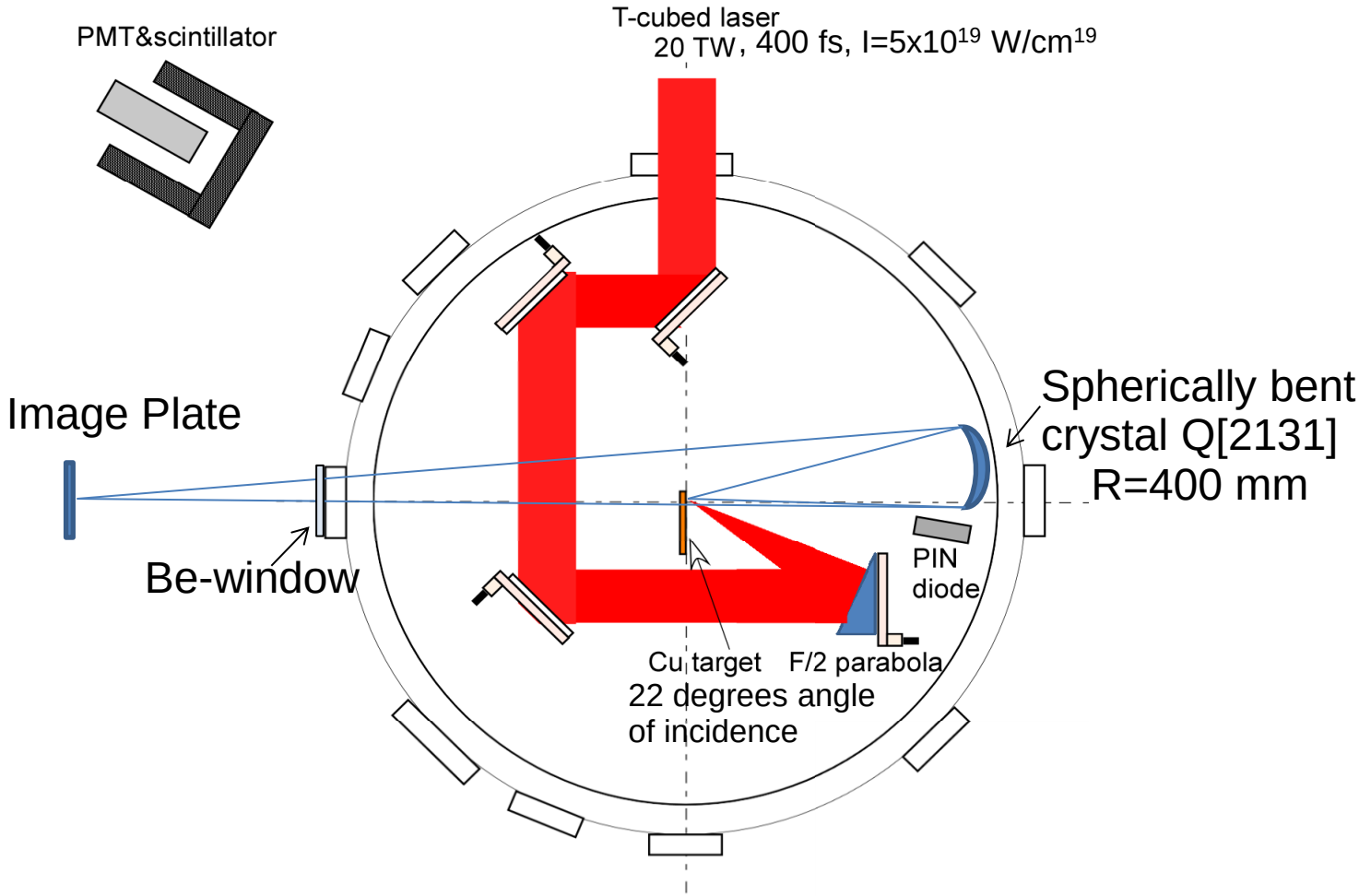

Bragg condition

$$n\lambda = 2d\sin\theta$$

Source wavelength

Cu K_α λ=1.541 Å

Q[2131] lattice spacing

2d=3.082 Å

Order of reflection

n=2

Bragg angle

θ=88.7 degrees

Integrated reflectivity

R=0.079 mrad

Geometry:

a=248 mm, b=1118 mm, M=4.5^x

Experimental setup for Cu K_α imaging

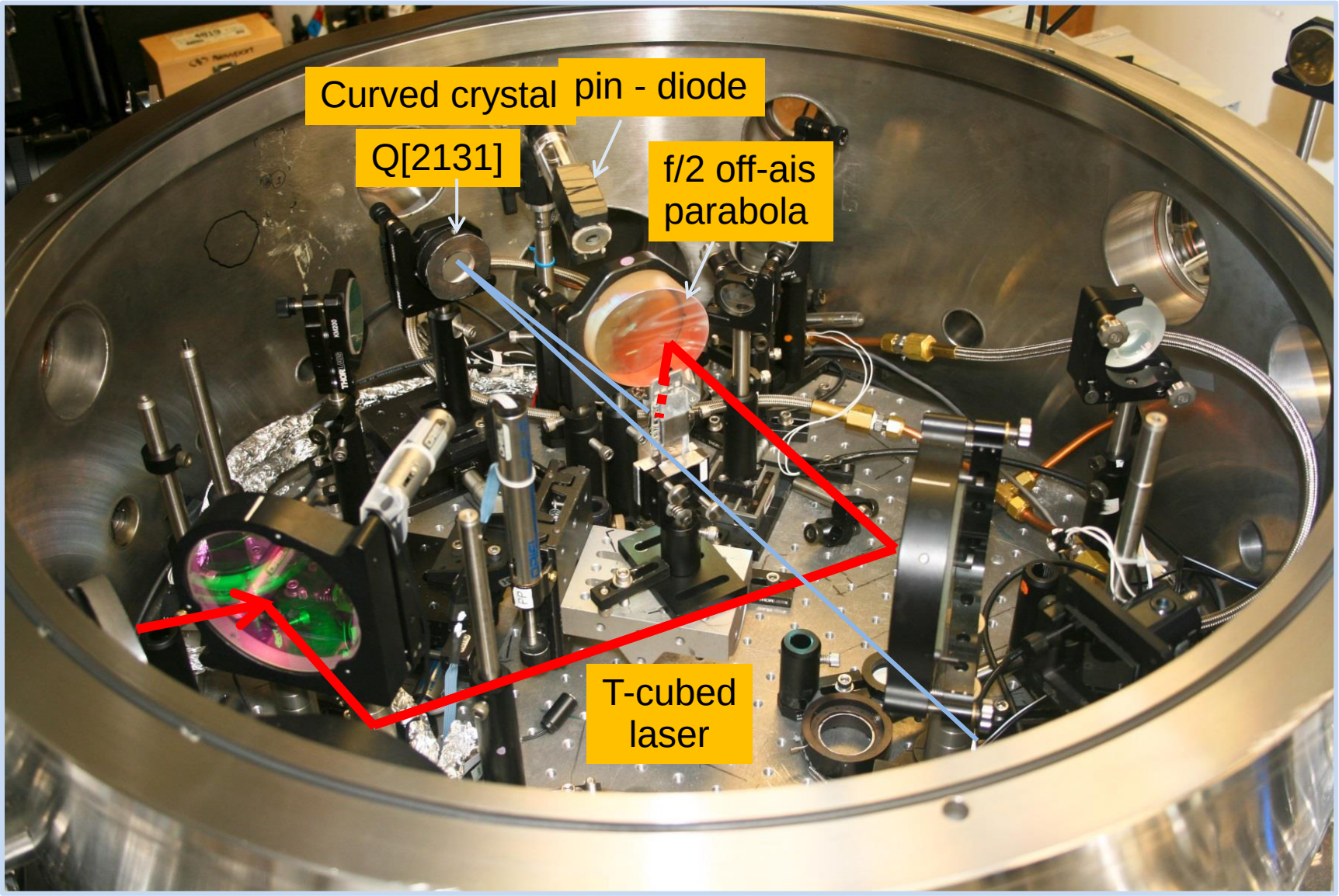

Obtain two focal spots with “Split parabolic mirror” and deformable mirror

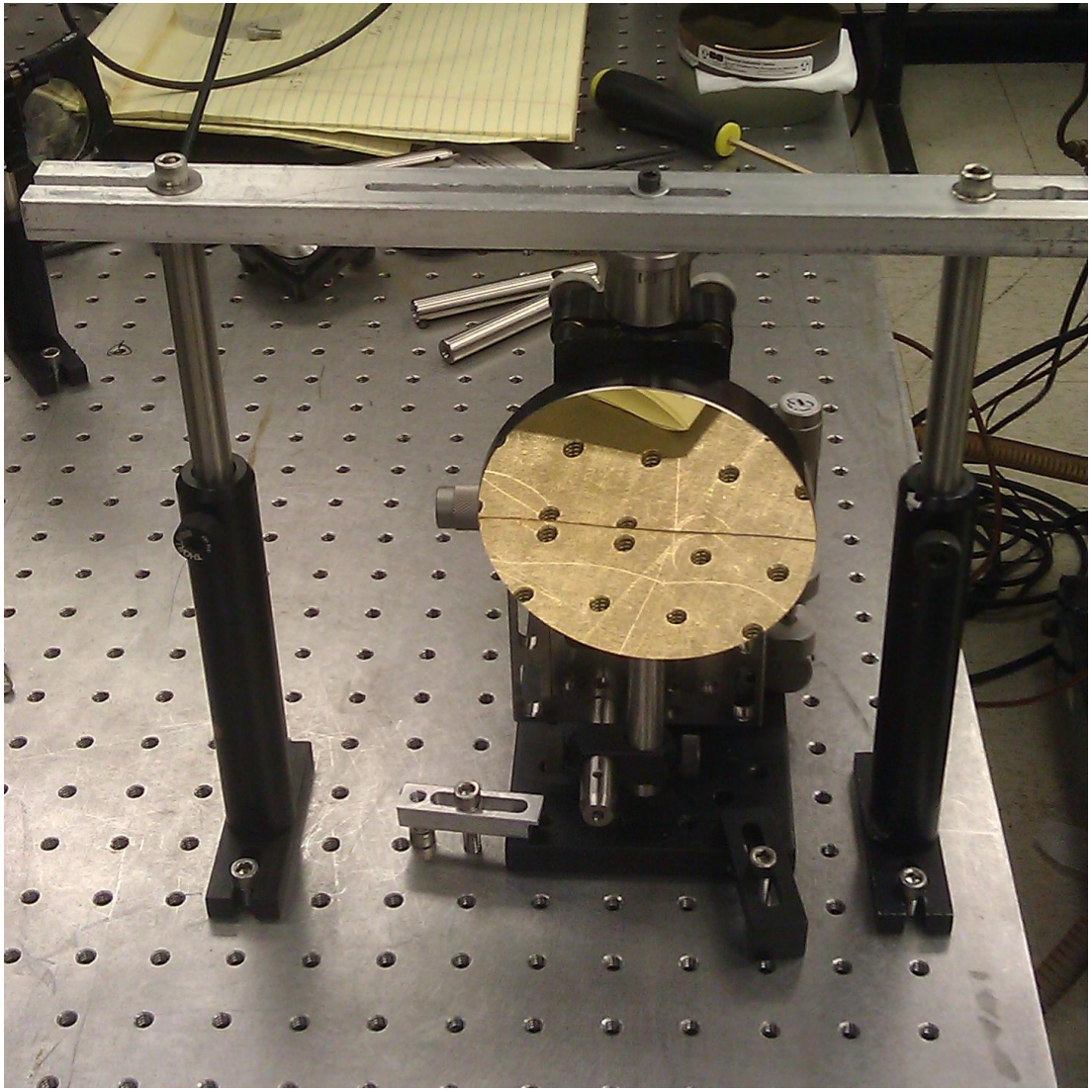

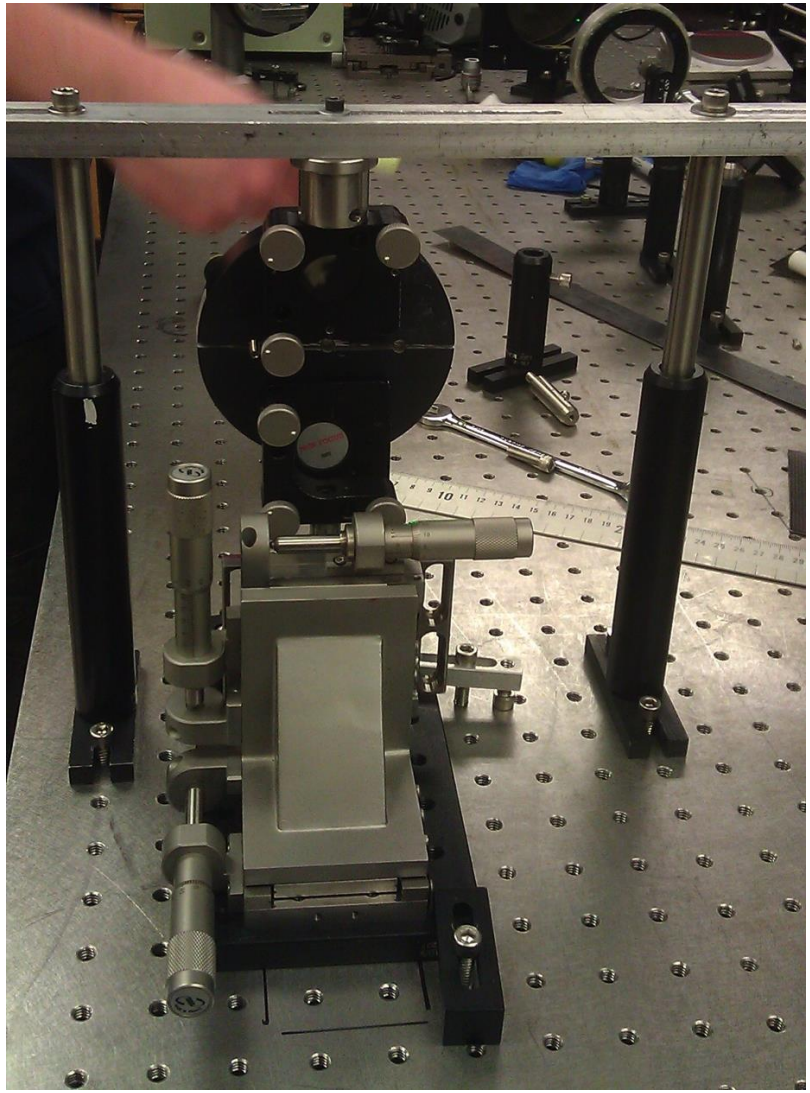

Sets up reconnection geometry with relativistic laser pulses (> 10^{19} W/cm^2)

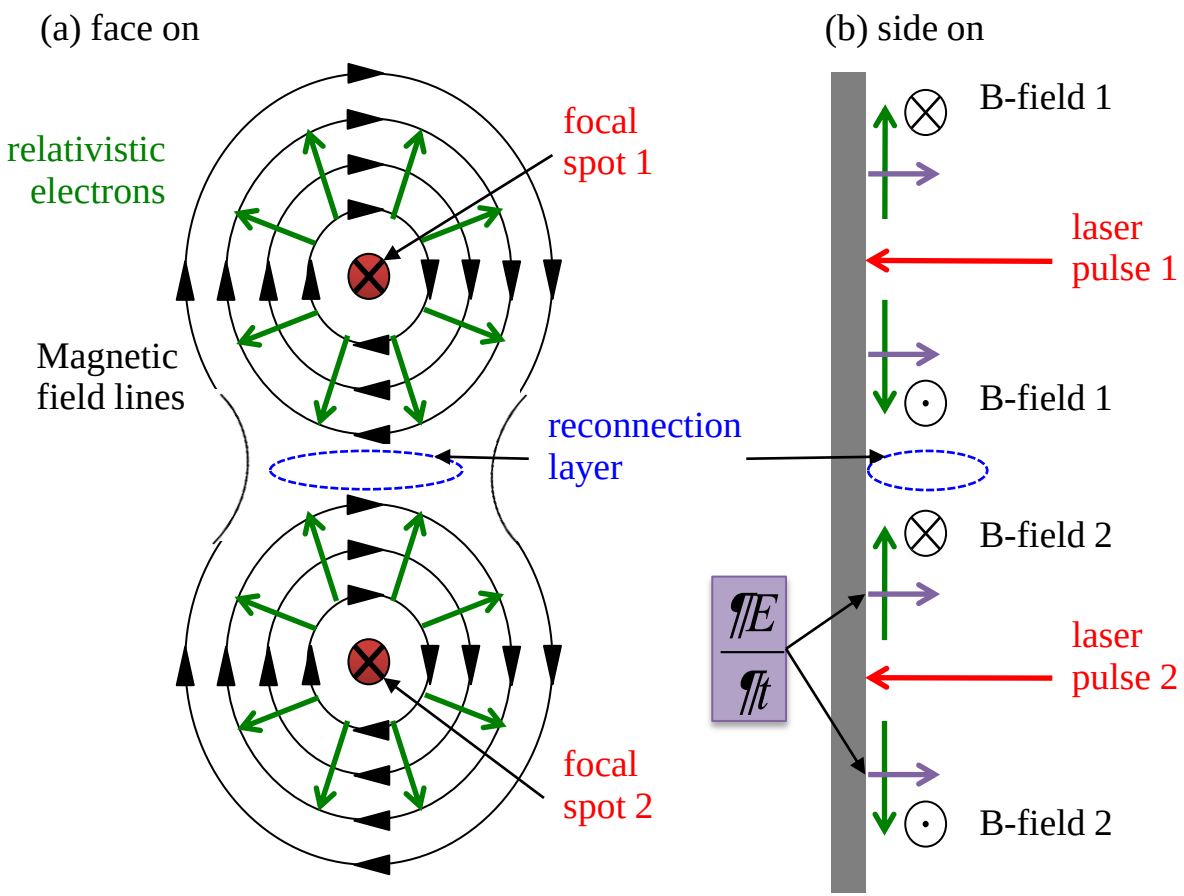

K-alpha imaging to diagnose reconnection

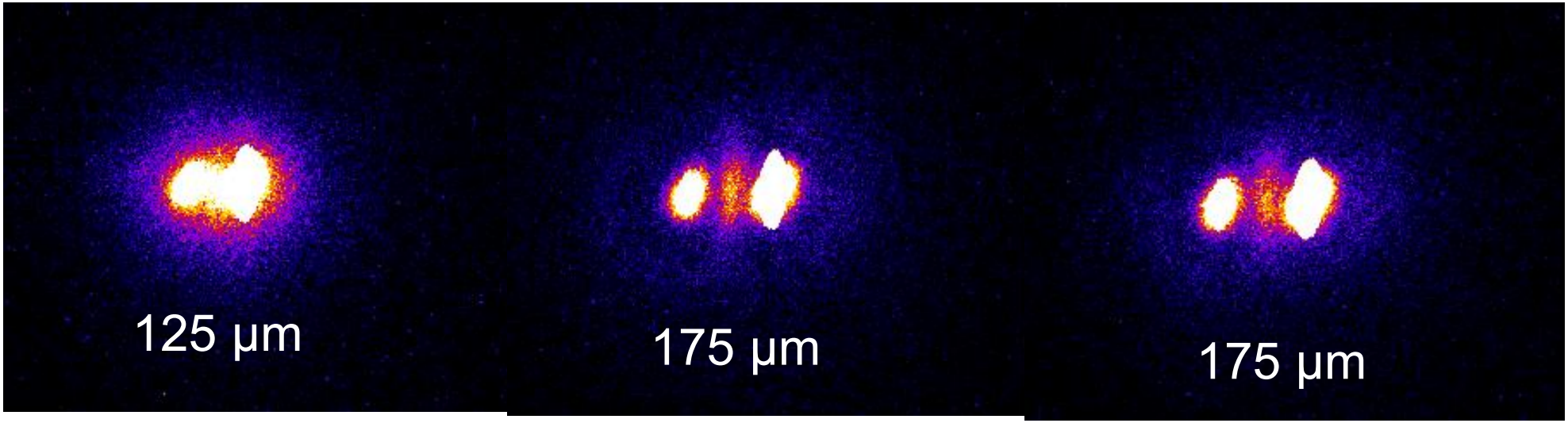

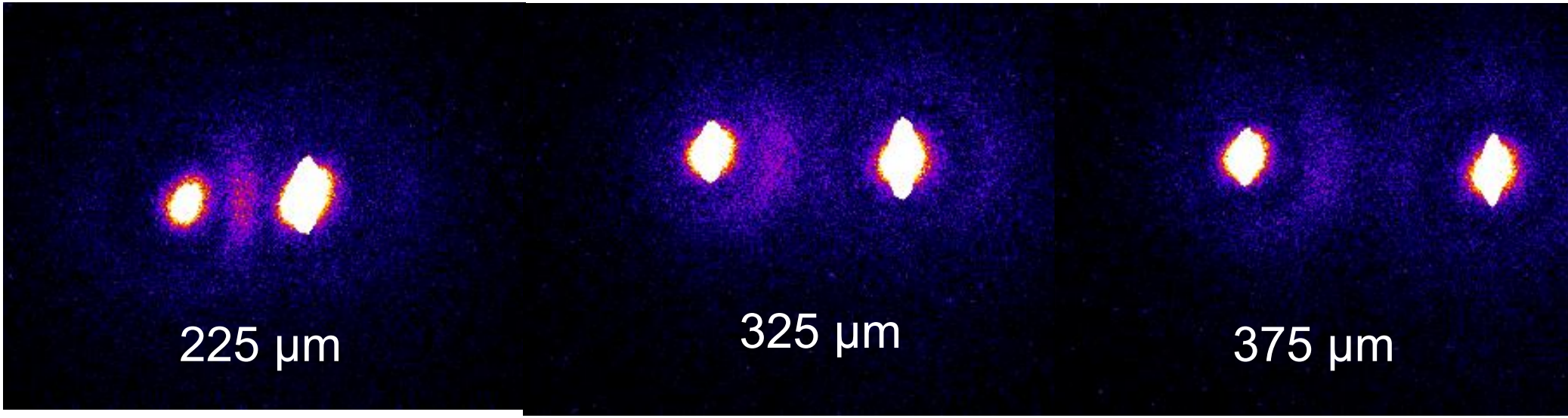

Measurement of plasma jets from reconnection ?

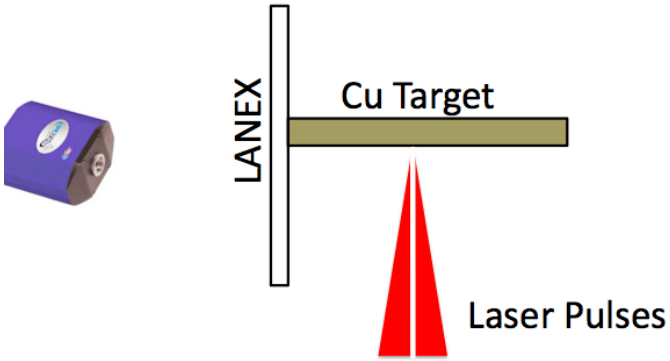

Electrons > 100 keV.

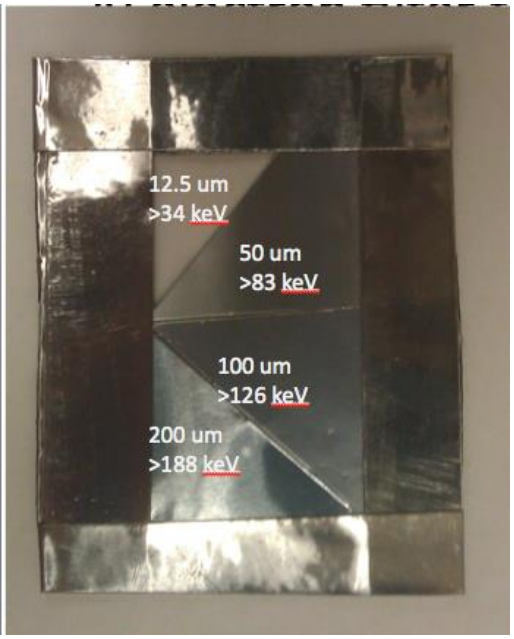

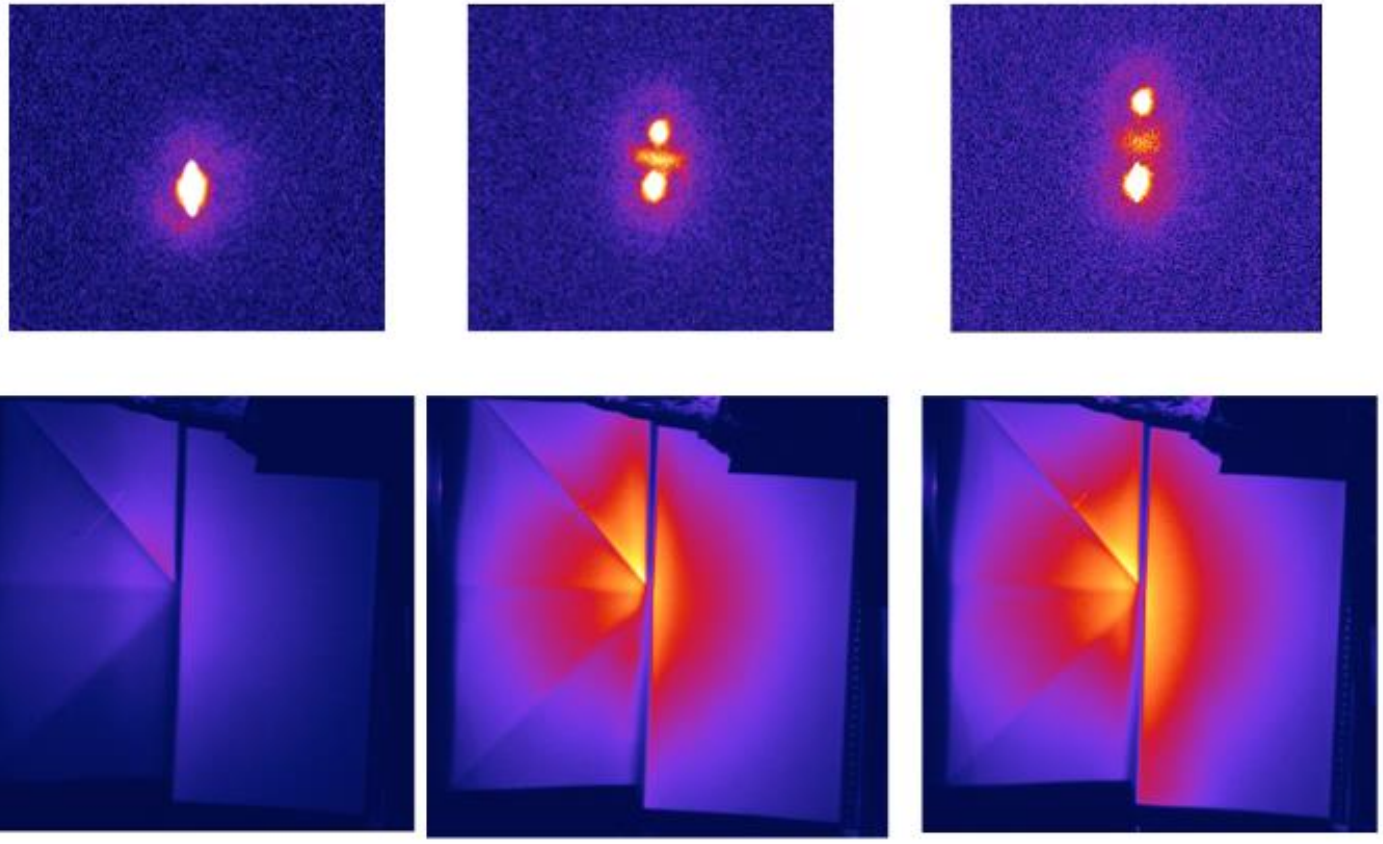

Use OMEGA EP with 500 J and 1000 J in 20 psec pulses – similar results

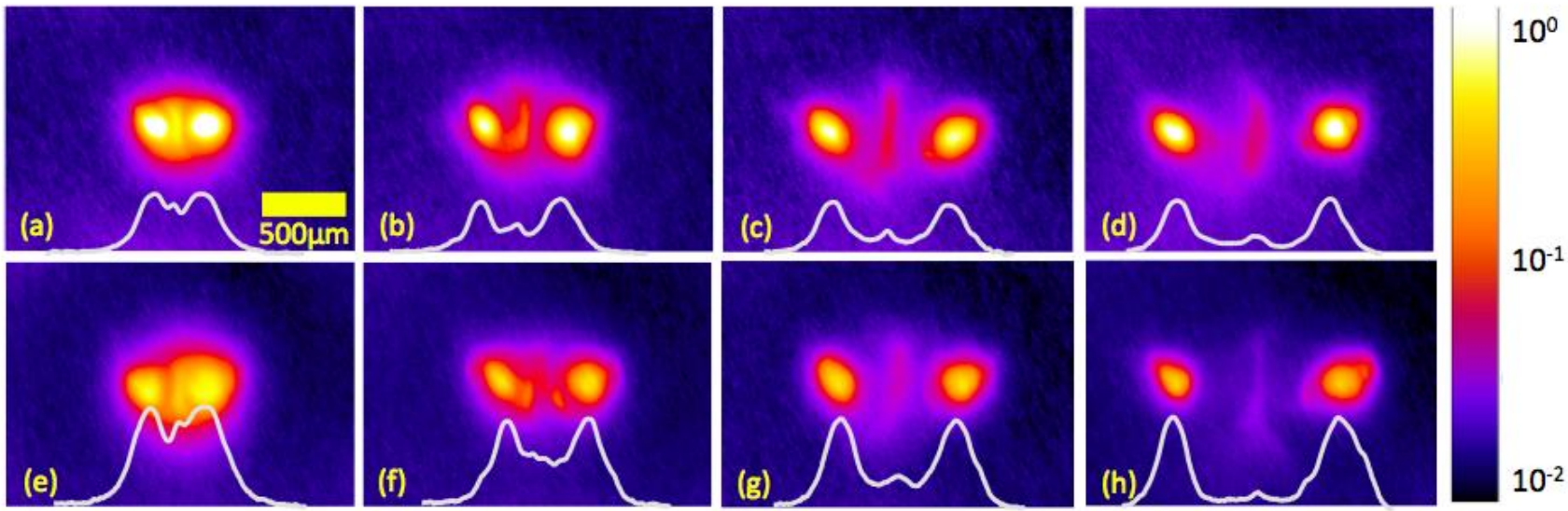

1000 J

500 J

250µm 500µm 750µm 1000µm

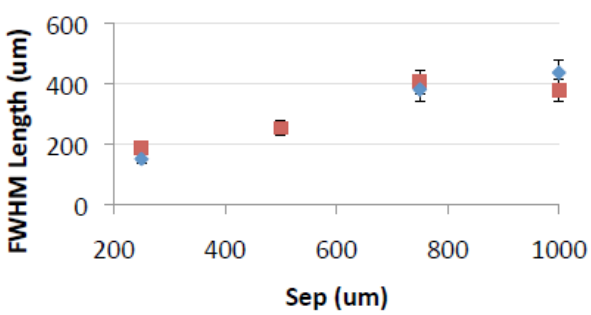

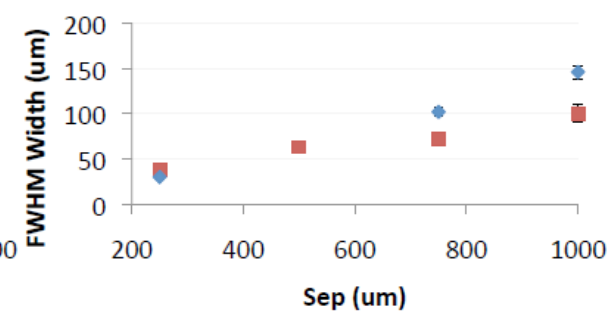

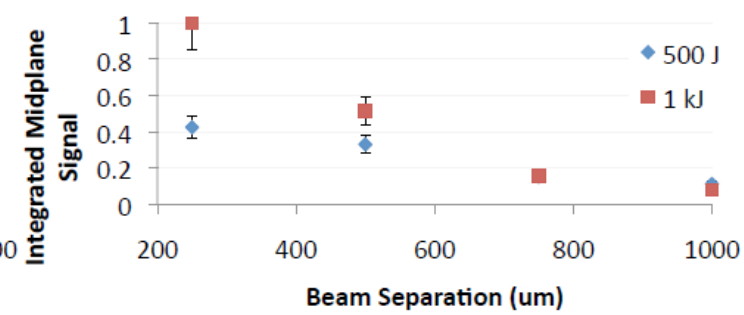

Temporal duration of mid plane signal from OMEGA EP

2mm x 3mm
Al

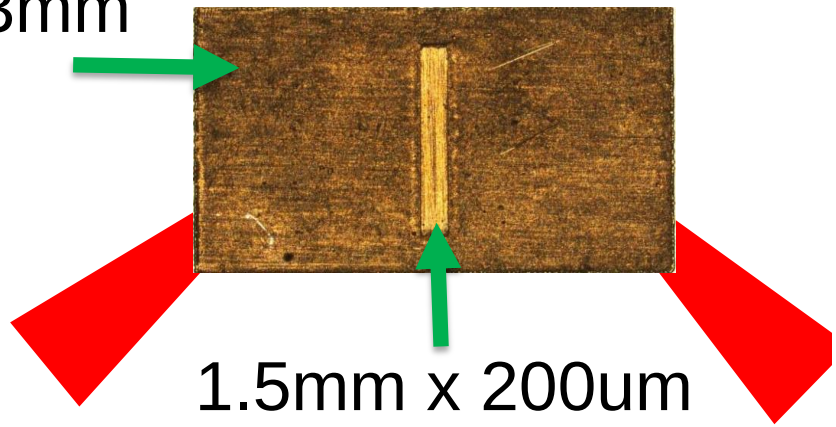

1.5mm x 200um
Cu bar

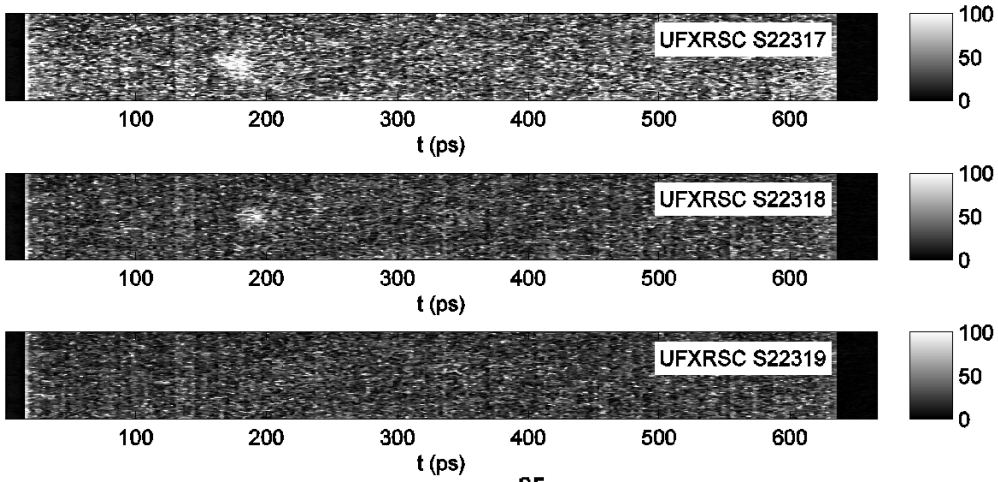

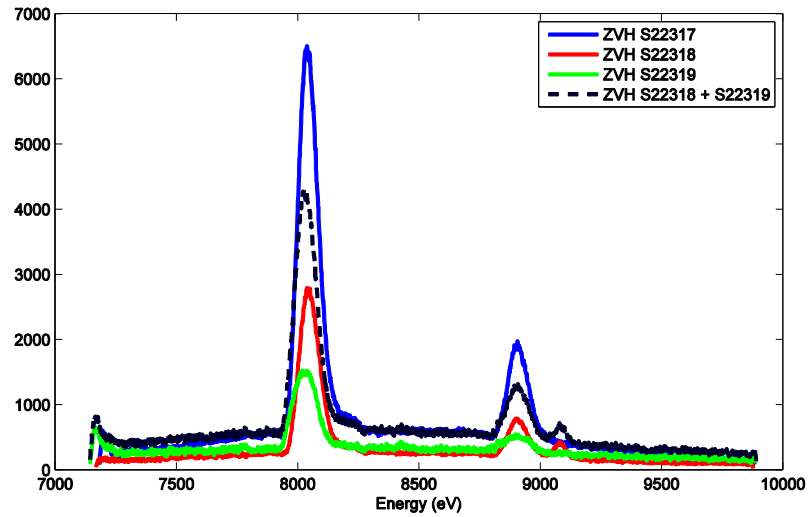

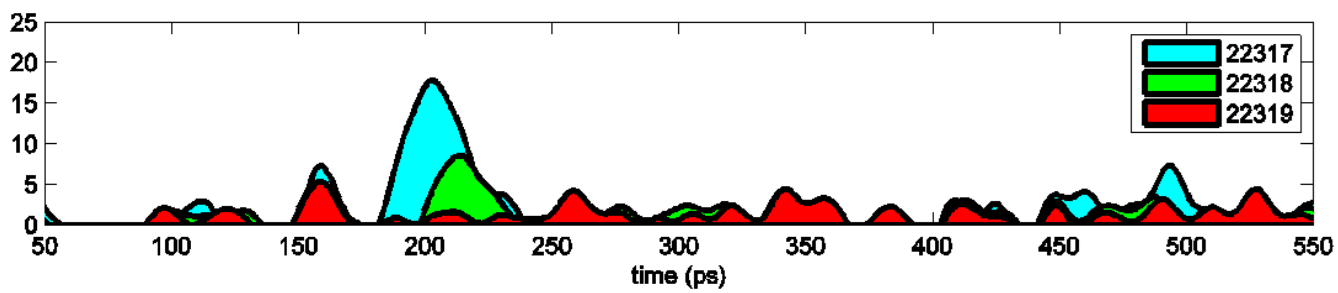

Simulations of reconnection geometry show E-field enhancement

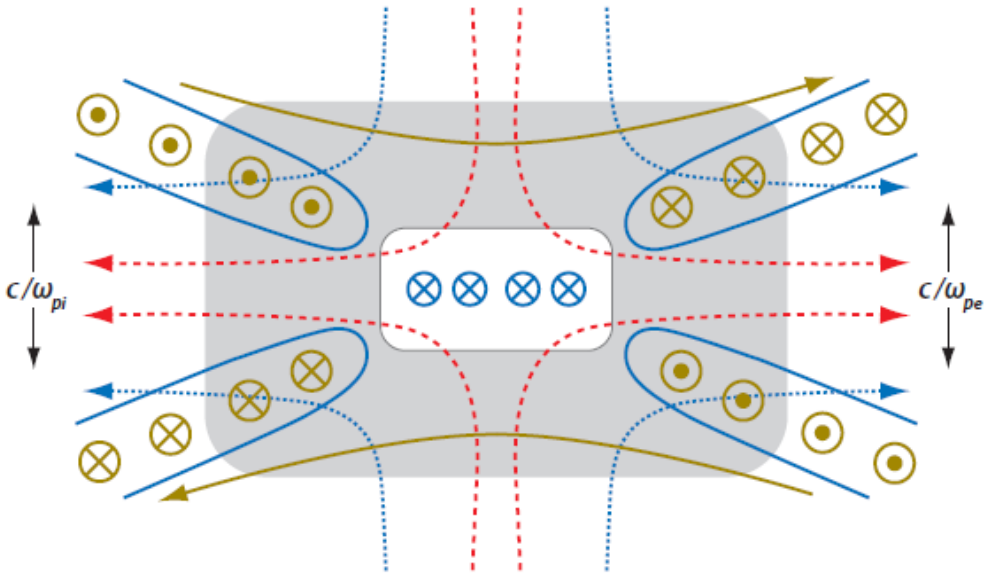

Phase space plot
- transverse momentum versus position

Laser interaction

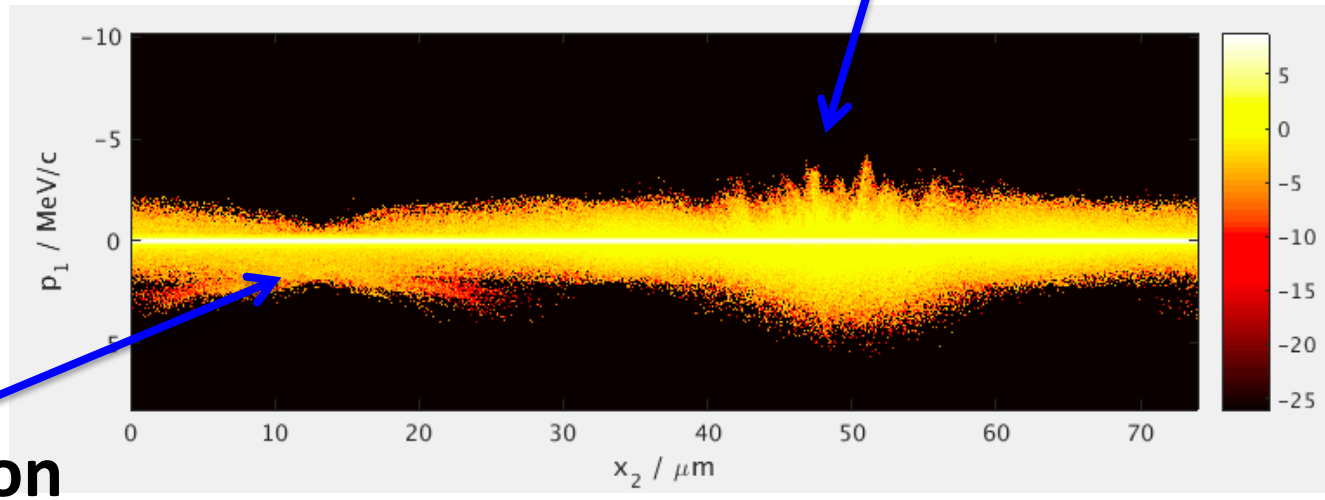

Reconnection

Pion production from Laser Wakefield Acceleration

Can we produce "exotic" particles like pions?
(Hercules and Astra-Gemini)

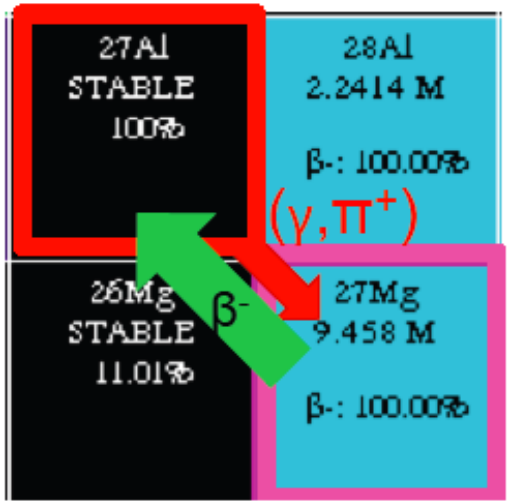

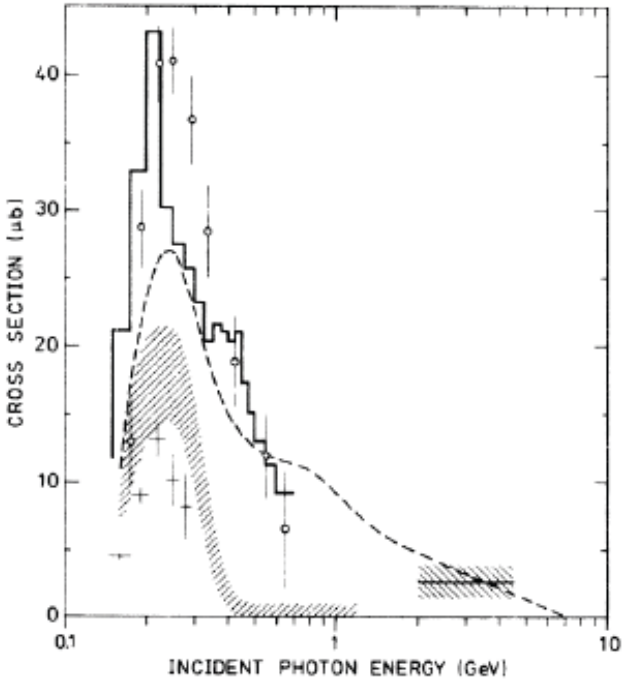

$^{27}Al(\gamma,\pi^{+})^{27}Mg$

- 140 MeV γ threshold
- 20 microbarn at 220 MeV γ

- ^{27}Mg is radioactive
  - 9.46 minute half-life
  - β^- emitter (843.7keV, 71.8%)
  - β^- emitter (1014.5keV, 28.2%)

Possible reactions and pathways

- Interactions yielding ^{27}Mg
  - (γ,π^+): $^{27}Al + \gamma \rightarrow {}^{27}Mg$
  - (n,p): $^{27}Al + n^0 \rightarrow {}^{27}Mg + p^+$
  - (n,abs): $^{27}Mg + n^0 \rightarrow {}^{27}Mg$
    - ^{27}Mg is radioactive with 9.46 min half-life (843 keV + 1014 keV)
- Additional trace interactions
  - (n,p): $^{56}Fe + n^0 \rightarrow {}^{56}Mn + p^+$
    - ^{56}Mn is radioactive with 2.58 hour half-life (846 keV + 1810 keV)
  - (n,p): $^{28}Si + n^0 \rightarrow {}^{28}Al + p^+$
    - ^{28}Al is radioactive with 2.24 min half-life (1778 keV)
  - Trace ^{40}K
    - ^{40}K is radioactive with 10^9 year half-life (1460 keV)

(γ,n) Neutron & (γ,π⁺) Pion Measurements

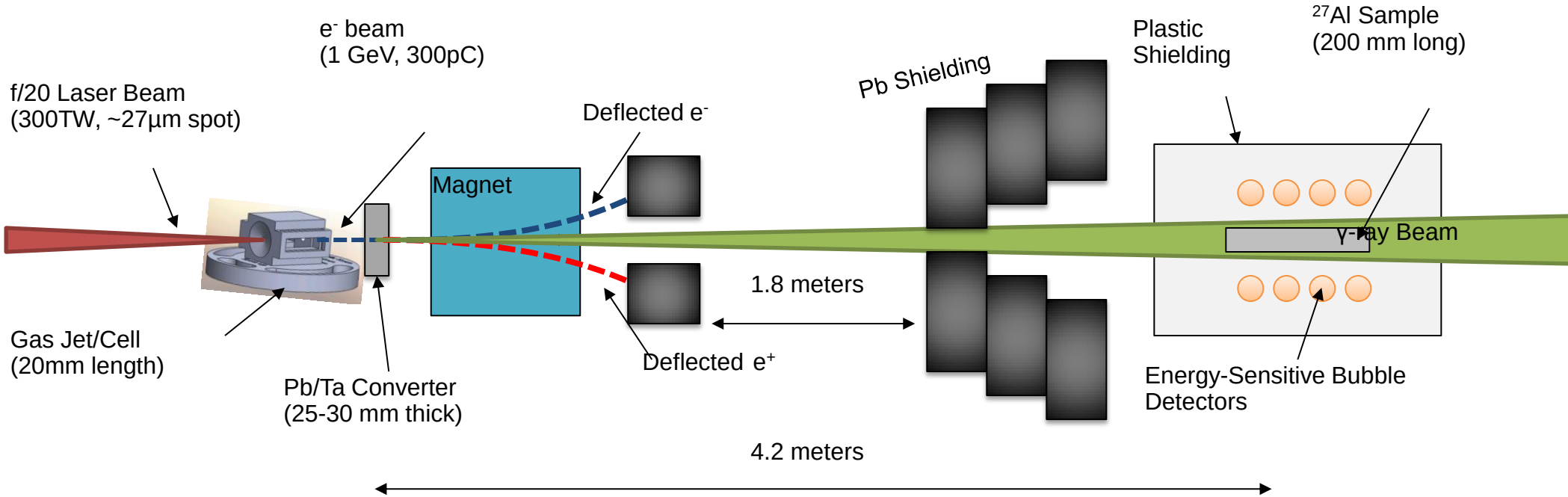

- Bubble detectors measured 5 (±3) x 10^6 neutrons/shot above 2.5 MeV
  - Roughly 5 x 10^5 neutrons/shot above 10 MeV (low energy neutrons attenuated by plastic)
- ^{27}Al activation estimates photo-neutron and photo-pion production
  - ^{27}Al (γ,n) ^{26}Al, where ^{26}Al is β+ emitter (511 keV signature) with long half-live, 13 MeV threshold
  - ^{27}Al (γ,π⁺) ^{27}Mg, where ^{27}Mg emits 843 keV signature with 10 min half-life, 140 MeV threshold

Neutron measurements

- Bubble detectors were placed adjacent to Al rod
  - Fluence for entire run (50 shots): 100000 neutrons/cm^2 (>2.5 MeV)
  - Fluence for "average" shot: 2000 neutrons/shot/cm^2 (>2.5 MeV)
  - Fluence for "average" shot: 1300 neutrons/shot/cm^2 (>10 MeV)

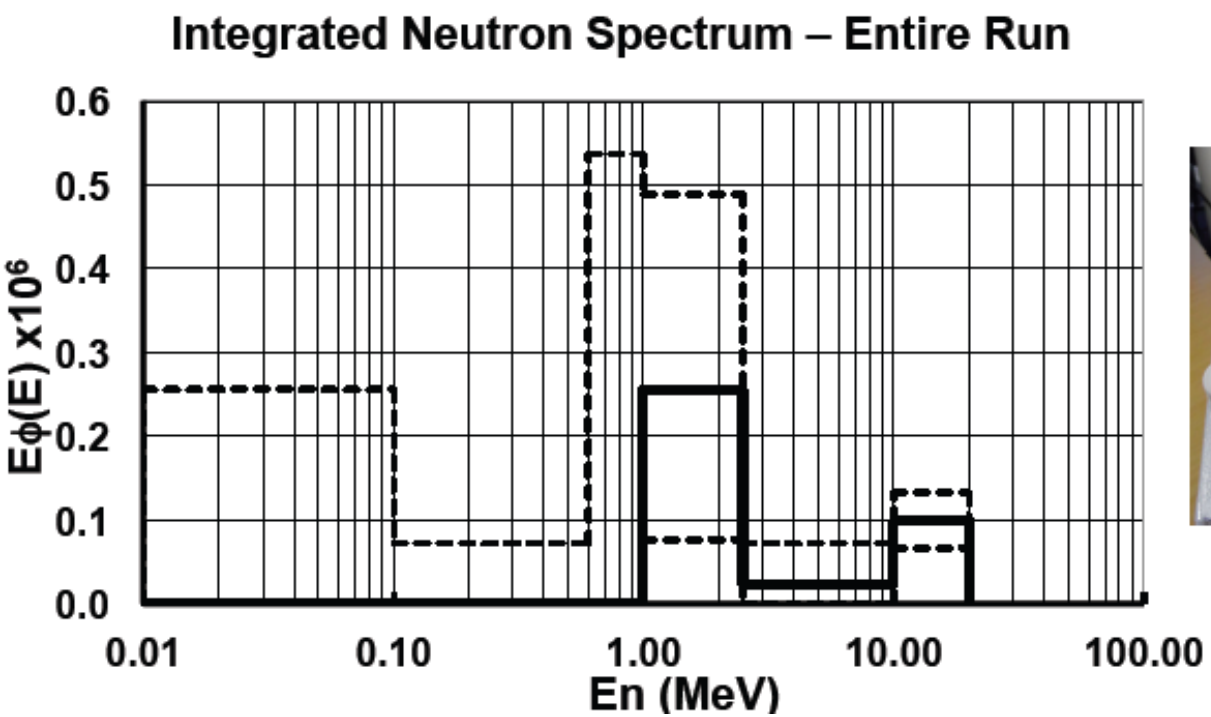

(γ,n) Neutron Divergence Measurements

- Low-energy bubble detectors
  - 5 times more neutrons in inner ring
  - 2 times expected from geometry
  - Implies low-energy "beam" of 75°
- High-energy (>10 MeV) bubble detectors
  - No neutrons in outer ring
  - Inner ring observed significant signal (20 bubbles)
  - Implies high-energy beam divergence is < 30°

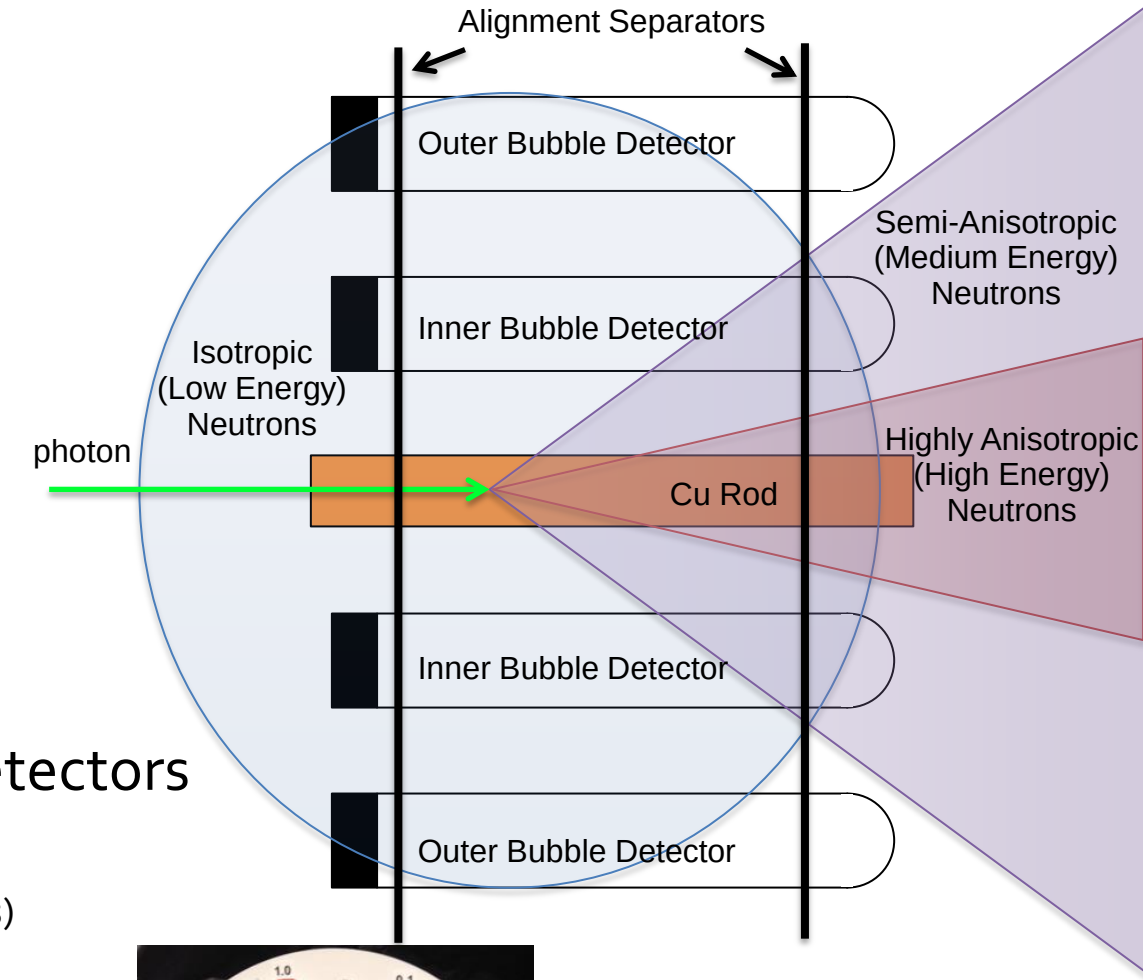

Activation measurements

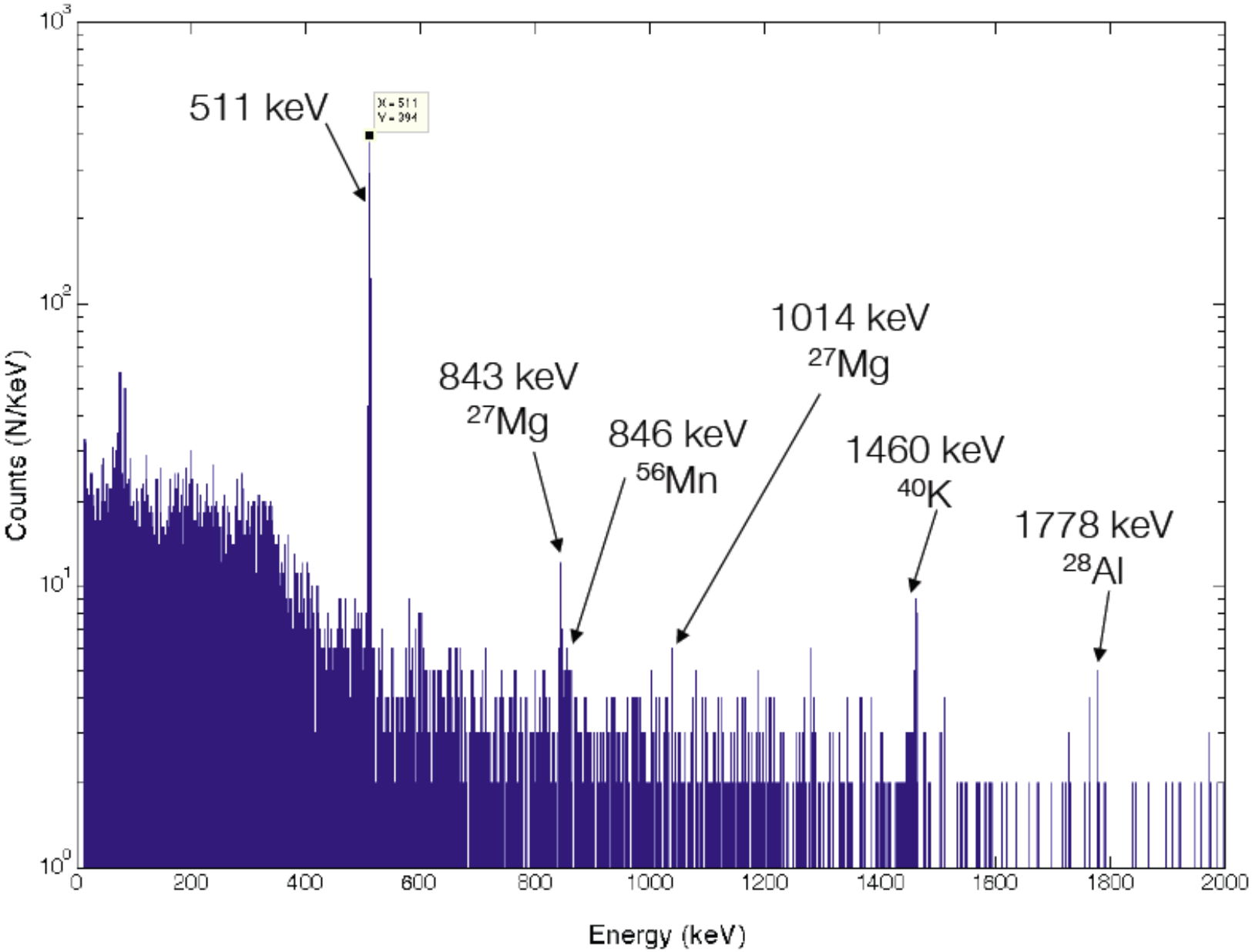

Evidence of "table-top" pion production!

- Experimental Measurements
  - HPGe detector
    - 843 keV – **25 counts -> 180 ^{27}Mg/shot**
    - 1014 keV – **6 counts -> 110 ^{27}Mg/shot**
  - **Bubble detectors**
    - 2000 neutrons/cm^2/shot >2.5 MeV **->** 3.75 **^{27}Mg/shot (estimated)**

Monte Carlo simulations (GEANT4/MCNP) agree with experiments
~ 100-200 pions generated per shot

Summary

- Betatron emission for x-ray generation can be controlled using laser/plasma parameters

- Betatron emission can be used for femtosecond absorption spectroscopy or dense plasma – and phase contrast imaging!

- K-alpha imaging is a useful diagnostic for reconnection driven by relativistic electrons

- Energetic electrons from laser wakefield acceleration can produce "exotic" particles,
  pions on a table-top

Recent Publications (DOE/NNSA Project)

1) High Flux Femtosecond X-ray Emission from Controlled Transverse Injection in a Laser Wakefield Accelerator,
T. Z. Zhao, K. Behm, C. F. Dong, X. Davoine, S. Y. Kalmykov, V. Petrov, V. Chvykov, P. Cummings, B. Hou, A. Maksimchuk, J. A. Nees, V. Yanovsky, A. G. R. Thomas, and K. Krushelnick (submitted 2015)

2) Ionization Injection Effects in X-ray Spectra Generated by Betatron Oscillations in a Laser Wakefield Accelerator
K. Behm, T.Z. Zhao, A. Maksimchuk, J. Nees, V. Yanovsky, K. Krushelnick, A.G.R. Thomas. J.M. Cole, J. Wood, S.P.D. Mangles (*Plasma Physics and Controlled Fusion* 2016)

3) Characterization of Hard X-ray Sources Produced via the Interaction of Relativistic Femtosecond Laser Pulses with Metallic Targets
T. Z. Zhao, T. Batson, B. Hou, J. Nees, A. G. R. Thomas, and K. Krushelnick (*Physics of Plasmas* 2016)

4) Characterization of Electrons and X-rays Produced using Chirped Laser Pulses in a Laser Wakefield Accelerator
T. Z. Zhao, K. Behm, A. Maksimchuk, J. Nees, V. Yanovsky, A. G. R. Thomas, and K. Krushelnick (*Plasma Physics and Controlled Fusion* 2016)

5) Radiation pressure absorption during high intensity interactions with solid density targets
F. Dollar, C. Zulick, A. Raymond, V. Chvykov, L. Willingale, V. Yanovsky, A. Maksimchuk, A. G. R. Thomas, and K. Krushelnick (submitted 2015)

6) Surface Limited Target Effects on Electron Dynamics with Femtosecond Laser Plasma Interactions
C. Zulick, A. Raymond, A. McKelvey, V. Chvykov, A. Maksimchuk, A. G. R. Thomas, L. Willingale, V. Yanovsky, and K. Krushelnick (submitted 2015)

7) Measurements of Ultrafast Magnetic Reconnection Driven by Relativistic Electrons
A. Raymond, A. McKelvey, C. Zulick, A. Maksimchuk, A. G. R. Thomas, L. Willingale, V. Chykov, V. Yanovsky, K. Krushelnick (submitted 2015)

End